TITLE:

Beyond ERCs: exploring catastrophic forms of rDNA instability in aging yeast

AUTHORS:

Joseph O. Armstrong*, Elizabeth X. Kwan*[1], Gina M. Alvino, M. K. Raghuraman, Maitreya J. Dunham, Bonita J. Brewer

Department of Genome Sciences, University of Washington, Seattle, WA

*Co-first authors

[1]Current address: Seattle Children's Research Institute, Seattle, WA

ABSTRACT:

Single-celled organisms grown in identical conditions have variable life spans. Identifying the factors that drive the inherent variability in life span is crucial for our understanding of aging at a fundamental level. Here, we revisit the role of chromosome XII instability as a source of life span variability in aging populations of the budding yeast, *Saccharomyces cerevisiae*. We followed populations of mother cells as they aged and quantified changes in karyotype, DNA content, and aberrant DNA structures, including the production of extrachromosomal rDNA circles (ERCs). We found that cells massively amplified their rDNA both as ERCs and as a structural form that could not be resolved on CHEF gels. We propose a model describing how these unresolved structures are generated. Our model, which we call CICR (Catastrophic IntraChromosomal Recombination), describes the consequences of recombination between repeats of different replication status. At the completion of replication, when all other replication forks have successfully terminated, CICR events leave behind a

single, unopposed replication fork in a branched form of Chr XII that has profound consequences during mitosis and/or subsequent cycles. This form of instability within the ribosomal DNA can lead to a myriad of toxic recombination products that may contribute to the life span variability in isogenic populations of aging yeast.

AUTHOR SUMMARY:

Aging is an uphill battle against entropy. The wear and tear on biological processes in cells require surveillance mechanisms and repair processes to stave off the inevitable. A cell's genome is constantly under external and internal insults that can ultimately lead to death. Known events that impact a cell's DNA are damage from free radicals (produced by the very oxygen needed for survival), shortening of the caps on chromosomes (called telomeres) every time a cell divides, and mutations that accumulate over time that affect essential cell processes. Yeast is an excellent tool to examine specific causes of aging because of its asymmetric mode of cell division: a mother cell can divide a limited, but variable number of times before senescing. We have isolated cohorts of mother cells, examined their genomes over the course of their life span and find a new intrinsic insult that the genome must endure. We find, in addition to the accumulation of extrachromosomal copies of the genes that encode the RNA portion of ribosomes (rDNA), that cells accumulate a toxic product of genetic recombination within the rDNA. The chromosome that contains the rDNA becomes branched and/or fragmented which leads to cell death.

INTRODUCTION:

Replicative life span (RLS) in the budding yeast *Saccharomyces cerevisiae* is defined as the number of daughter cells a mother cell can produce before senescing (Mortimer

46 and Johnson, 1959). Life span is under genetic control as specific mutations
47 significantly increase or decrease life span. Yet, in a population of genetically identical
48 cells, individual cells experience variable life spans. An attractive hypothesis for the
49 mechanism of yeast replicative aging, first proposed by Sinclair and Guarente (1997),
50 centered on the observation that aging cells accumulate additional rDNA copies, which
51 they suggested were entirely due to the accumulation of extrachromosomal rDNA
52 circles (ERCs). If accumulation of extrachromosomal circles reduces life span, it follows
53 that mother cells which form ERCs early in life would have a greater effect on life span
54 than mothers who form an ERC later in life. Consistent with this hypothesis is the
55 observation that mutations in genes involved in the replication and maintenance of the
56 rDNA locus alter ERC accumulation and life span (such as *fob1Δ* and *sir2Δ*; Defossez et
57 al., 1999; Kaeberlein et al., 1999, respectively). It was these findings that popularized the
58 notion that variation in life span among otherwise genetically identical cells could be
59 due to variation in their number of ERCs.

60 While ERCs are generally thought to be a key contributor to life span, a broader
61 rDNA theory of aging proposes that general instability in the rDNA is a root cause of
62 aging (Kobayashi, 2008). There are multiple aspects of the structure, replication and
63 transcription of the yeast rDNA locus that could contribute to its inherent instability.
64 First, the rDNA locus is made up of ~150 identical 9.1 kb repeats, each with a potential
65 origin of replication and the coding sequences for the four rRNAs (Fig 1A). The
66 tandemly repeated nature of the rDNA locus makes it prone to copy number changes at
67 a much higher rate than the rest of the genome (Supp Fig 1). Second, it is the most
68 highly transcribed region of the yeast genome; however, many of the copies are kept
69 silent by the histone deacetylase encoded by *SIR2* (Fig 1B; Aparicio et al., 1991). Third,

70 while the rest of the genome is replicated by bidirectionally oriented forks, the fates of
71 the bidirectional forks initiated in the rDNA are not equivalent: most of the replication
72 is unidirectional by a fork moving in the direction of 35S transcription (Fig 1C; Brewer
73 and Fangman, 1988; Linskens and Huberman, 1988). The oppositely oriented fork
74 proceeding into the 3′ end of the adjacent 35S transcription unit is arrested at a site
75 called the replication fork barrier (RFB; Brewer and Fangman, 1988) by the binding of
76 the Fob1 protein (Fig 1B,C; Kobayashi and Horiuchi, 1996).

77 The primary model to explain rDNA instability depends on breakage and repair
78 of the stalled replication fork resulting in a single-ended, double stranded break at the
79 RFB (Supp. Fig 2A; Kobayashi et al., 1998). Repair of this break is then thought to lead
80 to copy number changes within the chromosomal array and to the formation of an ERC.
81 This proposal is supported by observations that the *fob1Δ* mutant, which fails to arrest
82 forks at the RFB, is known to have a longer RLS and to produce fewer ERCs. However,
83 repair of the 3′ end of the broken fork, either by break induced replication (BIR., Supp
84 Fig 2B,E; Kramara et al., 2018; Li et al., 2026) or replication fork restart (RFR, Supp Fig
85 2C,F; Amiama-Roig et al., 2025) reestablishes a fork only to be blocked immediately by
86 Fob1 at the RFB (Supp Fig 2B,C) and does not directly produce an ERC.

87 The generation of ERCs is more easily explained by intrachromatid (pop-out)
88 recombination between repeats (but not interchromatid recombination; Supp Fig 2D,G).
89 If pop-out recombination were the primary mechanism of ERC formation, how might
90 *fob1Δ* mutants lead to a reduction in ERCs and an increase in RLS? In addition to its
91 fork blocking function, Fob1 also plays a role in stimulating recombination rates
92 regardless of the orientation of the RFB with respect to replication (Ward et al., 2000) as
93 well as by facilitating chromosome kissing (Choudhury et al., 2015), a process that

94 brings repeats into proximity. We propose, therefore, that ERCs are mainly formed by
95 pop-out recombination (Supp Fig 2G) independent of fork breakage.

96 To re-explore the mechanisms of rDNA instability we observed the aging
97 genomes of a population of mother cells for wild type and two mutants (*fob1Δ* and
98 *sir2Δ*) that differ in both RLS and stability of rDNA copy number. To study the kinetics
99 of rDNA instability we analyzed genome karyotypes by contour-clamped
100 homogeneous electric field (CHEF) gel electrophoresis and Southern blotting across the
101 replicative life span of these populations. In addition to analyzing karyotypes of the
102 aging populations, we also measured DNA content and cell cycle progression in
103 individual cells using flow cytometry. We tracked the progression of our time course
104 by measuring the viability of aging mothers using a membrane permeable stain and by
105 measuring the age of individual mother cells within the populations by counting bud
106 scars.

107 We observed increases to rDNA copy number in an age and genotype specific
108 manner that are non-uniformly distributed among individual cells in aging
109 populations. We identified that most of the additional rDNA copies were unable to
110 migrate during electrophoresis and remained in the well of the CHEF gel. We propose
111 that a significant portion of these non-migrating rDNA copies are the result of
112 Catastrophic IntraChromosomal Recombination (CICR, pronounced "sicker") between
113 rDNA repeats that differ in replication status and we generated a mechanistic model
114 that describes various outcomes of this catastrophic event. We propose that rDNA
115 instability manifests in aging populations in two ways: by CICR events that generate
116 toxic Chr XII recombination products and by pop-out recombination that generates
117 ERCs. These two forms of rDNA instability lead to different consequences in the

118 subsequent cell cycles, with each possibility having its own potentially unique impact
119 on the life span of individuals in aging populations.

120 **RESULTS:**

121 **Karyotyping the aging genome**:

122 We karyotyped the genomes of wild type, *fob1*Δ and *sir2*Δ populations
123 throughout their replicative life span. *FOB1* and *SIR2* are two of the best studied genes
124 in the field of yeast aging and provide context into high (*sir2*Δ) and low (*fob1*Δ) levels of
125 rDNA copy number variability with respect to wild-type populations. We used
126 miniature aging chemostat devices (MADs, Fig 2A; Hendrickson et al., 2018) to cultivate
127 the large populations needed for karyotyping by CHEF gel electrophoresis. We
128 assessed viability using a membrane permeable stain and flow cytometry (n > 10,000,
129 Fig 2B) and we quantified the replicative age of the populations over time by staining
130 and manually counting bud scars (n = 40, Fig 2C). We observed that *fob1Δ* mother cells
131 accumulated the highest average number of bud scars (mean: 19.4) and maintained
132 viability the longest of the three populations, while *sir2Δ* mother cells accumulated the
133 lowest average bud scars (mean 10.4) and exhibited more rapid loss in viability. These
134 results align with previously reported effects of *FOB1* and *SIR2* deletions on life span
135 (Defossez et al, 1999; Kaeberlein et al., 1999). The maximum replicative age observed
136 for each genotype occurred on different days (*fob1Δ*, day 6; WT, day 4; *sir2*Δ, day 3; Fig
137 2C). The mean replicative age of the wild type and *sir2*Δ populations slightly decreased
138 after reaching a maximum, likely due to differences in cell cycle progression among
139 individual cells.

140 We periodically sampled from the chemostats over the replicative life span of
141 each population and prepared agarose plugs for karyotyping by CHEF gel
142 electrophoresis. The ethidium bromide-stained gels of two replicate sets of aging
143 populations can be seen in Fig 2D,E. Bands in the CHEF gels contain one or more
144 comigrating chromosomes, with Chr XII being the largest and least mobile. Over time,
145 we see the disappearance of Chr XII and the appearance of additional DNA species
146 both above and below the position of Chr XII. The most prominent of these additional
147 DNA species is the rapidly migrating DNA smear of DNA in the size range of 50 to 200
148 kb that appears between days 4 and 6 concurrently with the loss of viability.

149 **Characterizing rDNA structural forms**

150 To explore the apparent disappearance of full length Chr XII, we probed the
151 CHEF gels with two single copy probes, one from Chr IV as a control (*GAL3*; Fig 3A and
152 Supp Fig 3A) and one from Chr XII (*CDC45*; Fig 3B; Supp Fig 3B). For wild-type and
153 *fob1Δ* populations, Chr XII (*CDC45* probe) appears as a discrete band with diminishing
154 intensity over time, while for the *sir2Δ* mutant Chr XII appears as a broad distribution
155 of sizes that was only detectable in the initial inoculum. The quantity of mobile full-
156 length Chr XII declines with age in all strains. The smear of DNA in the size range of 50
157 to 200 kb contains Chr XII fragments and increases in intensity with age. When we
158 hybridized the CHEF blots with unique probes from other chromosomes, we found that
159 fragmented products are not limited to Chr XII but are found for all chromosomes
160 probed (Fig 3A; Supp Figs 3A,B; Supp Fig 4) suggesting that the fragmented DNA is
161 from dead cells. The relative abundance of fragmented DNA serves as a secondary
162 measure of a decline in cell viability (Supp Fig 5).

163 The gradual disappearance of the Chr XII band also coincides with the
164 appearance of species of slowly migrating DNA between the well and the position of
165 Chr XII (Fig 2D,E). However, the slowly migrating species do not hybridize to the
166 *CDC45* probe and thus are not an intact form of Chr XII (Fig 3B; Supp Fig 3B). To
167 determine whether the DNA bands migrating slower than Chr XII contained rDNA, we
168 hybridized the CHEF gel blot with a probe from the nontranscribed portion of the
169 rDNA repeat (*NTS2*; Fig 3C; Supp Fig 3C). We see an overall increase in *NTS2*
170 hybridization that is age and genotype specific and that the slowly migrating new
171 bands are rDNA specific. They appear and accumulate with age, along with additional,
172 faster migrating bands not easily seen in the ethidium bromide-stained gel.

173 We characterized the numerous structural forms of rDNA present in the aging
174 populations via their gel mobility. While linear molecule migration is affected by their
175 length alone, circular species are particularly sensitive to electrophoresis conditions
176 (voltage and agarose concentrations) and can exhibit variable migration patterns
177 depending on their size and whether they are nicked or supercoiled. Supercoiled
178 monomer circles are compact, while their nicked counter parts have an open
179 conformation that can be temporarily and repeatedly impaled on agarose spikes,
180 slowing down their migration. To determine the identity of the various *NTS2* bands we
181 analyzed the migration patterns of the resident yeast 2-micron (6.3 kb) plasmid that can
182 exist as monomer circles (supercoiled and nicked) and as concatemers and catenanes
183 with variable numbers of repeats. Hybridization with 2-micron's *FLP1* probe (Supp Fig
184 6A) revealed that the migration in CHEF gels of multimeric forms of 2-micron was
185 particularly aberrant, with migration rates similar to chromosomes more than 100 times
186 their mass (Fig 3D). Over the course of the 6 days, as DNA fragmentation occurs in

187 increasing subsets of cells, we see decreases in some bands (supercoils) and a reciprocal
188 increase in other sets of bands (nicked). On the final day (eg. *fob1Δ* day 6, Supp Fig 6A)
189 we see the appearance of bands that correspond to linear forms of the different 2-
190 micron concatemers. We see similar shifts in subsets of bands in the *NTS2* blot (eg. Fig
191 3C) allowing us to identify different forms of ERCs and to estimate their repeat number.
192 From this analysis we conclude that, in aging mother cells, the majority of the *NTS2*
193 signal migrating in the gel corresponds to ERCs containing between one and five rDNA
194 repeats.

195 As cells age the amount of *NTS2* signal in the well also drastically increases.
196 When hybridized with probes from 2-micron and other chromosomes, we see only a
197 modest increase of signal in the well (Supp Fig 6B; Fig 4A;Supp Fig 7) that likely results
198 from branched replication intermediates from cells in S phase. What is responsible for
199 the retention of rDNA in the wells of the CHEF gels (Fig 3C; Supp Fig 3C)?

200 **Quantifying age-related increases in rDNA species**

201 To quantify and compare increases in *NTS2* and *CDC45* signals with age, we
202 compared the total combined signal (well, extrachromosomal, intact Chr XII and
203 fragmented) with the combined signal from *GAL3* (well, intact chromosome IV and
204 fragmented) and plotted the increases as a fold-change relative to *GAL3* over time (Fig
205 4A). We calculated the rDNA copy number by multiplying the fold change by the
206 respective rDNA copy number of the starting populations (124 repeats for wild-type,
207 125 repeats for *fob1Δ*, 106 repeats for *sir2Δ*). The total magnitude of rDNA repeat
208 increase by day 4 is staggering, especially for the *sir2Δ* aging mothers. The average
209 increase (~24-fold) in rDNA content corresponds to an additional average of 23.1 Mb

210 (1.9 genome equivalents) of DNA per cell. The ~12-fold increase in wild type on day 4
211 is equivalent to 13.5 Mb (1.1 genome equivalents) of additional DNA per cell. The ~3-
212 fold increase in rDNA in the *fob1*Δ strain is equivalent to an additional 3.4 Mb of DNA
213 or ~0.3 genomes per cell. We compared mean RLS for days where we observed an
214 increase to RLS from the previous day (wild type : days 0 – 4, *fob1Δ* : days 1 - 6) and
215 plotted it against rDNA copy number. We found a high degree of fit to an exponential
216 increase for each of the three populations (Fig 4B). We quantified how the extra rDNA
217 copies were distributed based on their structural identity by comparing the product of
218 *NTS2* signal in a particular position (i.e., in the well, as an intact chromosome, as an
219 ERC or as fragmented signal) and the total *GAL3* signal for each day in all positions (Fig
220 4C). While we can clearly see an increase in ERC copy number in wild type and *sir2Δ*
221 populations, most of the additional rDNA copies did not migrate during
222 electrophoresis and were retained in the well (Fig 4C).

223 **Non-migrating rDNA species**

224 DNA molecules can be retained in the well of a CHEF gel for a variety of reasons.
225 If incomplete lysis were the case, we would expect the other chromosomes to show the
226 same pattern, but they do not (Fig 3A; Supp Fig 3A; Supp Fig 4). A second possibility is
227 that the non-mobile rDNA copies are due to the presence of ERCs larger than five
228 repeats. However, we would predict that the larger an ERC is, the more likely it would
229 be broken and produce a linear molecule upon death. We do not see signal in the range
230 of discrete linear molecules that would be indicative of broken ERCs larger than five
231 repeats (Fig 3C,E). A third possibility is that the well contains branched circles in the
232 process of replication. As a comparison, we again used 2-micron molecules which are
233 known to replicate once each S phase (Zakian et al., 1979). As cells transitioned from

234 mostly G1 (day 0) to asynchronously cycling (days 1-3) the proportion of 2-micron
235 retained in the well increased to 40-50% (Supp Fig 6B), consistent with the generation of
236 branched circular replication intermediates (Brewer and Fangman, 1987). If we assume
237 a similar relationship for replication intermediates among the ERC concatemers that we
238 observe in 2-micron concatemers, replicating ERCs can only account for ~50% of the
239 total well signal. What other process could generate branched forms of Chr XII that
240 contain a massive increase in copies of rDNA repeats?

241 **Catastrophic IntraChromsomal Recombination (CICR)**

242 As noted in the introduction, the most likely way to produce an ERC is through
243 intramolecular pop-out recombination (Supp Fig 2G). Because homologous
244 recombination is cell cycle regulated and in haploid yeast occurs primarily in S/G2,
245 (Branzei and Foiani, 2008), we considered the consequences of recombination occurring
246 in S phase between repeats that differ in replication status (Fig. 5A,B). A model
247 proposed by Bruce Futcher (1986) to explain the amplification of the 2-micron plasmid
248 involves recombination between repeats that differ in replication status (Supp Fig 8)
249 and was the inspiration for our model. Recombination between the 2-micron's inverted
250 repeats in 2-micron that differ in replication status converts the bidirectionally
251 orientated replication forks into two forks that are moving in the same direction around
252 the 2-micron circle. Instead of terminating at a site opposite the origin, the two forks are
253 unopposed and continue copying the plasmid multiple times without requiring a new
254 round of replication initiation.

255 While the repeats of the rDNA locus are in direct orientation (the 2-micron
256 repeats are inverted) we considered the fate of replication forks when repeats that differ

257 in replication were to occur. Because replication initiation events in the rDNA are
258 scattered across the entire locus with approximately one in five of the origins being
259 active and the other nearby origins being passively replicated (Fig 1; Brewer and
260 Fangman, 1988; Linskens and Huberman, 1988), this interspersion of active and inactive
261 origins creates many opportunities for replicated repeats to interact with nearby
262 unreplicated repeats.

263 There are two possible orientations for interactions between a replicated and an
264 unreplicated rDNA repeat on the same chromatid. First, consider recombination
265 between a centromere proximal repeat that is in a replicated state and a distal repeat
266 that has not yet been replicated (Fig 5A). After resolution of the cross-over, one of the
267 products terminates with a closed, single-stranded loop of rDNA repeats hybridized to
268 a linear tail that extends through the centromere to the left telomere. The junction
269 between the loop and the tail is a replication fork that is blocked at the RFB. The
270 circular portion and the branch of the lariat structure could cause the retention of this
271 molecule in the well. Immediately after resolution of the recombination event, the other
272 product appears to be an intact linear form of chromosome XII; however, it is an
273 incompletely replicated molecule. After S-phase (Fig 5B) a single unopposed replication
274 fork remains in the rDNA in an orientation that would permit unimpeded replication of
275 centromere-proximal repeats leading to amplification of rDNA by a "runaway" fork.
276 We also expect the branched full-length chromosome to remain in the well during
277 electrophoresis.

278 The second possible interaction between a replicated and an unreplicated rDNA
279 repeat on the same chromatid is between a centromere-proximal unreplicated repeat
280 and a distal replicated repeat (Fig 5C). One of the products is again an rDNA lariat, this

281 time with the tail extending through the right telomere of chromosome XII. The branch
282 point between the circle and the tail is a fork in the permissive orientation for
283 replication ("rolling circle" fork), producing many tandem copies of the rDNA in a
284 process that extends the tail of the lariat. The reciprocal product, after the completion of
285 S phase (Fig 5D), would have a single branch point blocked at an RFB. In this
286 orientation the unopposed fork cannot be extended but would prevent the branched
287 chromosome from migrating out of the well.

288 Eukaryotic chromosome replication occurs by the establishment of multiple,
289 bidirectionally oriented replication forks. CICR events upset the balance of equal
290 numbers of left- and right-oriented replication forks. After a CICR event, when all of
291 the other forks in the genome have terminated replication by meeting an opposing fork,
292 there remains a single unopposed fork, either as a rolling circle fork or a runaway fork
293 which can continue to produce many additional copies of the rDNA repeats producing
294 the excess *NTS2* hybridization we observe in the well (Fig 3C; Supp Fig 3C).

295 **Consequences of CICR**

296 We propose that CICR events are a form of rDNA instability that lead to the
297 formation of lariats and singly-branched Chr XII with profound and varied
298 consequences that could shorten the life spans of individual cells. At the end of S
299 phase, all portions of Chr XII will have been replicated (Fig 5B,D); however, they cannot
300 be equally distributed between the two sister chromatids. One chromatid extends from
301 a telomere to a loop in the rDNA and the other contains a full-length version of Chr XII
302 with a duplicated terminal branch arising from the rDNA.

303 As cells proceed into mitosis they would face several challenges (Fig 6). The
304 ongoing replication fork could trigger a checkpoint similar to the fate of cells
305 undergoing BIR (Liu et al., 2025) or cells that contain an artificial chromosome that is
306 deficient in replication origins (van Brabant and Buchanan et al., 2000). The branch
307 could also break and result in the triggering of a DNA damage checkpoint. In either
308 case, there would be a cell cycle arrest requiring repair or adaptation to the checkpoint
309 before the cell can continue into mitosis.

310 If the cell makes it into mitosis, there are several potential outcomes for
311 chromosome segregation. First, if the mother cell had undergone recombination
312 involving a proximal duplicated repeat completes mitosis (Fig 6A), that cell may retain
313 the lariat, in which case it would be a lethal event due to missing essential genes from
314 the right arm of the chromosome. Alternatively, if the mother cell retains the branched
315 molecule the structure would be self-perpetuating in future divisions—the inherited
316 branch junction can be resolved but a new branched structure to its right is generated.
317 This scenario sets up the possibility that Chr XII will remain branched and thus will
318 remain in the well of the CHEF gel. In addition, this cell would have a duplication of
319 much of the rDNA and all genes distal to the rDNA.

320 Second, if a mother cell that has undergone recombination involving an
321 unreplicated proximal repeat completes mitosis, the branched ChrXII will likely be
322 broken and additional unique outcomes could occur (Fig 6B), depending on the
323 segregation of the acentric, rolling circle lariat. Mother cells that inherit this lariat could
324 continue to amass extra rDNA repeats that would be retained in the well by virtue of
325 the lariat's branched structure. For either scenario (Fig 6A,B) the increase in total rDNA

326 copies could contribute to an increased likelihood of ERC production through popout
327 recombination in proportion to their elevated rDNA copy number.

328 **Predictions of the CICR model**

329 We predict that CICR events contribute approximately half of the non-mobile
330 rDNA copy number increase that we observe retained in the well of CHEF gels;
331 however, it is inherently difficult to distinguish replicating (non-mobile) ERCs from the
332 rolling-circle lariat and branched forms of Chr XII predicted by the CICR model. One
333 way to detect these forked structures is to cleave the DNA in the well and run it on a 2D
334 gel to look for on-going and blocked forks in the rDNA (Brewer and Fangman, 1988).
335 However, once the molecules are cleaved, we have no way of distinguishing normal
336 replication forks in the rDNA (of which there would be many) from the single forks that
337 are associated with the CICR model.

338 A second prediction of our model is that concurrent with rDNA accumulation,
339 some CICR events should lead to a copy number increase in the chromosomal region
340 distal to the rDNA as the mother cells aged (Fig 6A,B). We further expected that to
341 detect such a copy number change, we should have to focus our attention on the
342 chromosome XII material that was retained in the CHEF gel wells and appeared in the
343 degraded DNA as the populations aged.

344 Accordingly, we quantified and compared signals from the CHEF gel blots that
345 were probed with unique probes from both sides of the rDNA (*CDC45* and *MAS1*, to
346 the left and right of the rDNA, respectively, as shown in Fig 1A; Fig 3, Supp Fig 9). We
347 selected the days where the fraction of the fragmented DNA signal for *CDC45* could be
348 quantified reliably (≥8.5% of the total signal in the lane) and calculated the fraction of

349 total *CDC45* signal present in the different structural forms of chromosome XII (intact,
350 well, and fragmented; Fig 7A, Supp Fig 10A) as well as the *MAS1*/*CDC45* ratio for the
351 well and the fragmented DNA (Fig 7B, Supp Fig 10B). Note that the absolute ratios are
352 arbitrary, as they will depend on the specific activities of the different probes as well as
353 how long the blots were exposed to the phosphor screens. What we were testing was
354 whether the ratio increased with age of the population, as predicted by the CICR model.

355 Consistent with our prediction for the CICR model, we see an increase in
356 *MAS1*/*CDC45* ratio with population age in wild type and *fob1Δ*. Such an increase is not
357 obvious in *sir2*Δ, which may be a manifestation of the accelerated aging of that
358 population—the increase must have occurred earlier than our earliest days for which
359 we could quantify signal. Across all populations, we see that the ratio is greater for
360 fragmented DNA than it is for the well, suggesting that cells that have undergone a
361 CICR event do not persist for long. Across all genotypes and sample times the
362 fragmented ratios consistently range from 1.3 to 2.3-fold higher than the well ratios (Fig
363 7B, Supp Fig 10B). While we do not see a genotype specific magnitude difference
364 between the well and fragment ratios, we do see a difference in the timing of when the
365 fragmentation begins with *sir2Δ* being the earliest and *fob1Δ* being the latest.

366 To confirm that the increase in ratio was not limited to the *MAS1* gene region, we
367 repeated the aging experiment with wild type cells in quadruplicate, examining DNA
368 from mother cells recovered on days 2 and 4. In this experiment, the cells appeared to
369 age more rapidly as we found significant ERC accumulation by day 2 and nearly
370 complete loss of full length Chr XII by day 4 (Supp Fig 11A). We hybridized the four
371 replicates with *CDC45* and a sequence approximately 240 kb distal to *MAS1* that
372 contained the origin of replication *ARS1222* (Supp Fig 11B,C). On day 2, the ratio

373 among the fragmented DNA was nearly twice that of the DNA retained in the well (Fig
374 7C), a result consistent with the magnitude of the ratios found for *MAS1*/*CDC45* ratios
375 in the original two wild type replicates. By day 4, the ratio fell but was still greater than
376 the ratio in the well. In addition to the increases in the fragmented DNA, we also
377 found, between day 2 and day 4, a small but significant increase in the *ARS1222*/*CDC45*
378 ratio in the DNA retained in the well, a feature we had not detected with the *MAS1*
379 probe in the original two replicates of the wild type cells (Fig 7C). This latter finding is
380 also consistent with the CICR model that branched and lariat forms containing an extra
381 copy of the distal arm of Chr XII would be expected to be retained in the well.

382 In principle, bulk short read sequencing of aging mother cells could also reveal
383 copy number changes in the distal portion of chromosome XII. However, using
384 sequencing as the assay is challenging because it demands that the CICR events occur in
385 a large enough sub-population to be detectable by read depth changes. Furthermore,
386 unlike with CHEF gel analysis, we would not be able to assess read depth for the
387 molecules of interest (those in the wells and the breakdown products) vs. the
388 background of intact molecules. Nevertheless, we examined read depth across Chr XII
389 using short read sequencing on wild type mother cells from days 0 and 4. Perhaps
390 unsurprisingly, read depth profiles appeared identical, with the exception of a ~3-fold
391 increase in rDNA copy number between day 0 and day 4 populations (Supp Fig 12 A-
392 D). The fact that our Southern blot quantifications detected a 10-fold increase between
393 the same samples (Fig 4A) underscores the documented limitations of short read
394 sequencing in assessing copy numbers in repetitive DNA (Morton et al., 2020). Overall,
395 the results support key predictions of the CICR model of rDNA instability and its
396 potential role in yeast aging.

397 **Assessing the cause of death in aging populations**

398 To determine to what extent additional rDNA copies contributed to cell death we
399 used flow cytometry and the non-specific DNA stain Sytox green to assess cellular DNA
400 content across individual cells throughout the life span of our populations. We
401 generated cell cycle profiles on days 0 – 4 and 6 for each of the three populations (Fig
402 8A; Supp Fig 13A). These profiles consist of two main peaks, corresponding to the cells
403 in G1 and G2 phases, with S phase cells in between. The day 0 samples are enriched for
404 G1 cells because cells are deprived of nutrients for multiple hours during the magnetic
405 bead-labeling protocol. In the following days, there are clear G1 and G2 peaks, but
406 most notably, in the *sir2Δ* mutant and to a lesser extent in wild type cells, subsets of
407 cells were observed to contain more than two (and up to eight) genome equivalents of
408 DNA (Fig 8A; Supp Fig 13). We quantified the proportion of the cells that contain more
409 than 2 genome equivalents of DNA and find that more than 40% of the *sir2Δ* population
410 fell into this category by the end of life, and roughly 20% and 6% in wild type and *fob1Δ*,
411 respectively (Fig 8B). Because some cells in the G2 peak may actually be G1-arrested
412 cells with amplified rDNA, we may be underestimating the fraction of cells that have
413 experienced an amplification event. The subset of cells containing more than 2N
414 genomic content has an average genome size from 3.3 to 3.8 N, an increase in DNA
415 content per cell that is consistent with the level of excess rDNA repeats estimated in Fig
416 4A (an average of ~1.9 extra genome equivalents), but could also include extra copies of
417 the distal arm of Chr XII generated by CICR. The increase in genome content across all
418 three genotypes suggests that cells that experience an rDNA instability event succumb
419 to similar levels of DNA accumulation regardless of genotype and that the major way
420 these populations differ is in the frequency of the initiating event.

421 To determine whether the accumulation of additional rDNA was associated with
422 a loss of viability, we used fluorescence-activated cell sorting (FACS) to separate the
423 *sir2Δ* population into live cells and dead cells. The high efficiency of the sort can be
424 seen in the spot dilution series shown in Fig 8C. We then generated cell cycle profiles
425 for the live and dead populations and found that the non-viable population was more
426 likely to contain additional DNA (Fig 8D; Supp Fig 14). This finding suggests that the
427 additional rDNA copies generated either by unopposed replication forks or as ERCs are
428 associated with a reduced life span. However, it is important to note that among the
429 nonviable *sir2Δ* cells ~50% have died without accumulating additional DNA. These
430 cells may have died by a mechanism unrelated to rDNA instability or from inheriting
431 only the proximal or distal fragment of Chr XII produced during a CICR event (Fig
432 6A,B).

433 Finally, to assess whether unopposed replication forks generated by CICR events
434 contributed to cell death, we returned to the analysis of the ratios of *MAS1* or *ARS1222*
435 to *CDC45* among the fragmented DNA (Fig 7B,C; Supp Fig 10). Because these three
436 probes reside on the same chromosome, we would expect to see equivalent fractions in
437 the fragmented DNA if cells were dying from ERC accumulation. However, the ratios
438 in the fragmented DNA (*MAS1*/*CDC45* or *ARS1222*/*CDC45*) were nearly 2:1, indicating
439 that cells that contain an amplification of the distal arm of Chr XII were dying
440 preferentially relative to cells with the expected 1:1 ratio. Furthermore, the wild type
441 *ARS1222*/*CDC45* ratios declined by day 4, suggesting that cell death was now occurring
442 in cells with normal Chr XII by either ERC accumulation or some other event unrelated
443 to rDNA instability.

444 **DISCUSSION:**

445 We propose an alternative mechanism for rDNA instability that can generate
446 multiple forms of rDNA rearrangements that contribute to a shorter life span. Our
447 proposed mechanism, based on intrachromosomal (pop-out) recombination (Scherer
448 and Davis, 1979; Rothstein, 1983), can generate canonical ERCs when recombination
449 occurs between repeats in the same stage of replication (in G1 or G2 cell cycle phases).
450 When repeats of different replication status recombine (in S phase) the result is
451 potentially catastrophic for Chr XII and the cell. These recombination events (that we
452 have named CICR for Catastrophic IntraChromosomal Recombination) result in lariat
453 structures that terminate at one end in a telomere and a reciprocal product that is a form
454 of Chr XII with a branch point within the rDNA locus. In the mitosis following a CICR
455 event, the potential unequal parsing of regions of Chr XII adds an additional layer of
456 nuance to the relationship between rDNA instability and aging. Most cells in a
457 population faithfully complete replication; however, cells also have a small, but similar,
458 chance to form an ERC or undergo a CICR event at rates that are influenced by their
459 *SIR2* or *FOB1* genotypes (Supp Fig 16). The consequences of a CICR event differ from
460 an event that creates an ERC because ERCs need multiple cell cycles to accumulate to a
461 toxic level, while CICR events could have a more profound and acute effect on life span.
462 Immediately following a CICR event, cells may suffer from delays in cell division,
463 experience secondary effects of Chr XII segmental duplication, or die within one or a
464 few cell cycles as a result of the loss of essential genes from either the proximal or distal
465 arm of Chr XII (Fig 6A,B).

466 The CICR model can explain our genetic, molecular, and kinetic data and is
467 consistent with some of the literature on the involvement of rDNA instability in
468 replicative aging. Here we cite three relevant findings: First, in a strain with impaired

469 rDNA origins (*rARS-Δ3*; Hattori et al., 2022) ERC production in mothers (~7 divisions)
470 is significantly reduced yet the accumulation of additional rDNA species in the well of
471 the CHEF is comparable to that of wild type cells. This finding is consistent with the
472 proposal that the well-retained rDNA is not in the form of autonomously replicating
473 ERCs but some other form of branched DNA.

474 Second, a mutation in the histone acetyl transferase (*rtt109*) significantly shortens
475 RLS (Dang et al., 2009) and increases rDNA instability (Ide et al., 2013). Using atomic
476 force microscopy to examine DNA that remained in the well of a CHEF gel from the
477 *rtt109* mutant Ide et al. (2013) found lariat structures, with a loop size equal to roughly
478 one rDNA repeat, at a frequency of ~1% in the *rtt109* mutant and at a frequency of
479 <0.1% in wild type cells. They proposed the lariats arose as follows: "To initiate rolling
480 circle replication, the broken end at the RFB must recombine with . . . popped-out
481 circular molecules (ERC)." However, the fork that is established by this invasion event
482 is in the non-permissive orientation for replication with respect to the adjacent RFB and
483 we believe would be unlikely to form a rolling circle replicon.

484 Third, Zylstra et al. (2023) measured the DNA content of *rad52Δ* mutant cells at
485 the onset of senescence and found no ERCs but instead found, by whole genome
486 sequencing, a modest increase (up to ~1.6-fold) of the unique region of Chr XII between
487 the rDNA and the right telomere. While our finding of a similar fold increase in *MAS1*
488 relative to *CDC45* among the Chr XII fragments of aged mothers is consistent with their
489 finding, it is not clear how our explanation invoking CICR would be operating in a
490 *rad52* mutant. From sequence data they concluded that the extra sequences would
491 constitute a linear fragment of 1.8 Mb but provided no CHEF gel analysis of uncut
492 chromosomes to support this claim. We would suggest that if CICR had produced this

493 excess of Chr XII-right sequences these extra copies would be found either retained in
494 the well or among fragments of Chr XII released from dead cells.

495 There is also precedence in the literature for the basic feature of the CICR model
496 that proposes an unusual fate for intramolecular recombination that occurs between
497 repeats of different replication states. A model proposed by Bruce Futcher (1986; Supp
498 Fig 8) for the amplification of the 2-micron plasmid involves recombination between its
499 two inverted repeats, one replicated and the other unreplicated. The resolution of this
500 cross-over event converts the bidirectionally moving replication forks into two rolling
501 circle forks that chase each other around the plasmid spinning out multiple tandem
502 copies of the 6.3 kb repeat. This mechanism is catalyzed by the site-specific
503 recombinase, Flp1, which is induced when copy number of the 2-micron plasmid is low
504 (Murray et al., 1987). A second model by Johansson and Diffley (2021) proposes a
505 scenario involving DNA repair and replication fork restart that can result in DNA re-
506 replication. They did not specifically address issues at the rDNA, nor address the
507 consequences on chromosome segregation. However, when we apply their model to
508 the rDNA locus, we predict that it would generate a cell with two branched Chr XII
509 chromatids, one with a runaway fork (B2 in Figure 5B) and the other with a fork
510 blocked at an RFB (D2 in Figure 5D). The key similarities shared by this model, in
511 which a replicated segment recombines with a re-replicated segment, and the Futcher
512 and CICR models, are the creation of unopposed replication forks and the consequences
513 that this imbalance has on genome stability.

514 In this study we have focused our attention on recombination events in the
515 rDNA occurring *in cis* between repeats that differ in replication status and have
516 proposed that the initial consequence of these CICR events is the generation of

517 unopposed replication forks. Recombination *in trans*, i.e., between the rDNA locus and
518 ERCs, can also generate unopposed replication forks (Supp Fig 15A). Integration of an
519 ERC with an unfired origin or an ERC in the process of replication, into a region of the
520 rDNA that has already been duplicated, generates the potential for re-replication and
521 production of one runaway fork and a second fork blocked at the RFB. But in this case,
522 both forks are on the same chromatid, within the rDNA, oriented away from each other
523 (Supp Fig 15B). The consequences for chromosome integrity are not as dire since the
524 regions of Chr XII that are proximal and distal to the rDNA are not affected. In
525 particular, cell division, would not create gene imbalance or broken chromosomes.
526 While these events may add to the increase in rDNA copy number we find in the well of
527 mother cells as they age, they cannot be responsible for the increase in the *MAS1*/ or
528 *ARS1222*/*CDC45* ratios we find among the fragmented DNA from aging mothers.

529 rDNA instability and aging have largely been connected through the ERC
530 hypothesis; however, we propose that intrachromosomal recombination between rDNA
531 repeats of different replication states also contribute to rDNA instability by producing
532 aberrant forms of Chr XII that play a major role in the life span trajectories of individual
533 yeast cells. We believe this mechanistic model better captures the complex nature of the
534 relationship between rDNA instability and RLS.

535 **METHODS:**

536 *Strains used in this study :*

Wild-type (WT)	FY4 - *MATα*, *flo1*::KanMx, *flo9*::NatMx
*sir2*Δ	FY4 - *MATα*, *flo1*::KanMx, *flo9*::NatMx, *sir2*::KanMx
*fob1*Δ	FY4 - *MATα*, *flo1*::KanMx, *flo9*::NatMx, *fob1*::KanMx

537 Each of the strains used in this study contains deletion of two genes which
538 contribute to flocculation. The deletions of *FLO1* and *FLO9* facilitate the separation of
539 mother cells from daughter cells. Although the laboratory strain we used, FY4, is not
540 known to flocculate in standard synthetic growth media, flocculation can be induced in
541 laboratory strains with age (Hendrickson et al., 2018). We also attempted to keep rDNA
542 copy number consistent between the three strains by selecting transformants with
543 similar rDNA copy number to our WT strain.

544 *Magnetic labeling and cultivating aging yeast :*

545 Cultures derived from single cells were grown overnight in 2 mL synthetic
546 complete (SC) media containing 2% glucose. The overnight cultures were transferred
547 into 25 mL SC media and allowed to grow overnight until saturation. For each strain
548 and each replicate, 10^9 cells (~50 ODs) were isolated and washed five times in 5 mL
549 phosphate buffered saline (PBS) before being resuspended in 5 mL PBS + 30%
550 polyethylene glycol (PEG; w:v). To activate the carboxylate modified magnetic beads,
551 1-Ethyl-3-(3-dimethylaminopropyl)carbodiimide (0.091 g) and N-Hydroxyl succinimide
552 (0.541 g) were added to 2 mL MES buffer (1X) along with carboxylate modified
553 magnetic particles (Seramag speedbeads, 0.2 mL, washed twice in 0.5 mL MES). The
554 mixture was briefly sonicated before it was placed on an orbital shaker at room
555 temperature for 45 minutes. After the incubation, the beads were washed three times in
556 1 mL PBS (1x) and sonicated again before they were added to the yeast cells suspended
557 in PBS+30% PEG. The cells and beads mixtures were then placed on an orbital shaker
558 at room temperature for 45 minutes. The magnetically labeled cells were isolated with a
559 magnetic rack and washed five times in 25 mL SC media before being resuspended in
560 1mL SC media. A small aliquot (50 μL) of these cells was saved for characterization and

561 the remaining portion was loaded into two chemostats. The labeled cells were allowed
562 to adhere to the exterior magnets for 30 minutes before the media and air pumps were
563 turned on. SC medium was perfused into the cultures at a rate of ~33 mL hr^{-1} which
564 corresponds to a dilution rate of ~2 hr^{-1}. Air was filtered, hydrated and continuously
565 perfused into the chemostats using aquarium pumps. A second set of aging chemostats
566 was performed with the wild type strain and samples were collected on days 1-4.
567 Uneven loading of samples on the CHEF gels limited the karyotype analysis to days 2
568 and 4.

569 *Mother cell sampling and purification:*

570 The aging populations were sampled over a six day period by first stopping the
571 media and air pumps and vortexing the chemostats to free the cells from the walls of
572 the chemostat. At each sample time ~10^7 cells were isolated. The mother cells were
573 separated from the daughter cells using a benchtop magnet. Mother cells were washed
574 on the magnet five times with 1 mL PBS.

575 *Viability and bud scar quantification :*

576 Viability was approximated using the membrane permeability stain propidium
577 iodide. Briefly, 5 μL of propidum iodide (1 mg/mL) was added to 1 mL PBS containing
578 $5x10^5$ cells. Cells were left in the dark for 20 minutes before viability was assessed using
579 a C6 flow cytometer. For each sample >20,000 cells were measured. Cells were first
580 gated from the free magnetic particles and viability was assessed using the FL3 channel
581 (630 nm).

582 The average replicative age of the culture was assessed using wheat germ
583 agglutinin congugated to alexafluor 488 (WGA-488). $5x10^5$ fixed cells were washed in 1

584 mL PBS and sonicated before 5 μL 1 mg/mL WGA-488 was added and the culture was
585 left to stain for 20 minutes. The cells were centrifuged and resuspended in 20 μL PBS.
586 Z-stack images of the stained cells were collected using a Leica widefield microscope at
587 100x. The bud scars of 40 cells were quantified for each sample.

588 *Analysis of genomic DNA by CHEF gel electrophoresis and Southern blotting*

589 Mother cells retrieved from the aging chemostats were embedded in 1% GTG
590 low-melt agarose (10^7 cells for day 0 and $5x10^6$ cells for the remaining days in a 90 μl
591 plug). Genomic DNA was purified *in situ* according to Tsuchiyama et al. (2013). The
592 plugs were embedded in a 1% LE agarose gel and electrophoresis was carried out in 2.3
593 L of 0.5 × Tris Borate EDTA (circulating at 14˚C) using a Bio-Rad CHEF DR-II
594 electrophoresis cell. Conditions for electrophoresis that maximized the resolution of
595 Chr XII were 100 V for 68 hr, with a switch-time ramped from 300 to 900 sec (Kobayashi
596 et al., 1998). The gels were stained with Ethidium Bromide (0.3 μg/ml) for 30 minutes,
597 destained for 30 minutes and photographed with UV illumination. Southern blotting to
598 GeneScreen membranes and hybridization with ^{32}P-dATP labeled PCR probes were
599 carried out using standard protocols. We sequentially probed the blots with different
600 labeled fragments after stripping twice in boiling 0.1xSSC , 1% SDS. The probes
601 included fragments to unique sequences on Chr IV (*GAL3*), Chr XII (*CDC45*, *MAS1* and
602 *ARS1222*), Chr X (*ILM1*), Chr V (*CUP1*), and repeated sequences on 2-micron (*FLP1*) and
603 the rDNA (*NTS2*). To image and quantify the signal intensities of individual bands
604 and/or lanes, we exposed the blots to X-ray film and to Bio-Rad Molecular Imaging FX
605 phosphor, respectively. Phosphor screens were scanned using a Bio-Rad Personal
606 Molecular Imaging scanner and analyzed using Bio-Rad's Quantity One software.

607 *Live/dead sorting :*

608 To assess viability, 5 μL of propidum iodide (1 mg/mL) was added to 1 mL PBS
609 containing $5x10^5$ purified mother *sir2*Δ cells and incubated in the dark for 20 minutes.
610 The population viability was assessed to be ~40%. 100,000 cells assessed as dead by the
611 propidium iodide uptake were collected along with a fraction of 100,000 cells assigned
612 as live by the lack of fluorescence using a Sony MH800 fluorescence assisted cell sorter.
613 A series of 10-fold dilutions was spotted onto YPD plates to assess the efficacy of the
614 sort.

615 *Sytox green staining:*

616 At each sampling time ~10^5 cells were fixed in 70% ethanol. Cells were pelleted
617 and washed twice in 1 mL 50 mM sodium citrate, treated with RNase A (0.25 mg/mL)
618 and incubated at 50˚C for 1 hour. Cells were then treated with proteinase K (0.5
619 mg/mL) and incubated at 50˚C for an additional hour. Sytox green was added to the
620 samples which were stored at 4˚C until they were measured on a Becton Dickinson
621 Accuri C6 flow cytometer.

622 *Illumina sequencing and copy number quantification*

623 DNA was isolated from mother cells from days 0 and 4 using a phenol
624 chloroform extraction. DNA libraries were prepared using the Illumina DNA prep kit.
625 Whole genome sequencing was performed with a NextSeq 550. Copy number was
626 calculated by evaluating the average read depth over 1000 bp windows and normalized
627 to a ploidy of 1.

628 **FUNDING SOURCES:**

This project was supported by the Biological Mechanisms of Healthy Aging Training Grant (T32AG066574) to JA, by the University of Washington Nathan Shock Center of Excellence in Basic Biology of Aging (P30AG013280) to MJD and by National Institutes of Health (https://www.nih.gov) grant R35 GM122497 to BJB and MKR. MJD holds the William H. Gates III Endowed Chair in Biomedical Science.

ACKNOWLEDGMENTS:

The authors would like to thank Lorraine Symington and Bruce Futcher for helpful discussions, Josh Cuperus for reading an early version of the manuscript, Bruce Futcher for insightful comments on this version of the manuscript, Rebecca Martin for help with Southern probes, and Kelsey Zane for copy editing.

FIGURE LEGENDS:

Figure 1: Structure, transcription, and replication of the rDNA locus on Chr XII
A) The rDNA locus is found on the 2.5 Mb Chr XII and is composed of ~150 copies of the 9.1 kb rDNA repeating unit. Each unit is identical in sequence and encodes two transcripts (35S and 5S), a potential origin of replication, and a replication fork barrier (RFB). The nontranscribed spacers (*NTS1* and *2*) contain multiple regulatory sequences. *NTS2*, the unique genes *CDC45* and *MAS1* and the origin of replication *ARS1222* are used as hybridization probes in this work. B) The Sir2 deacetylase silences 35S transcription (blue triangles) in roughly half of the rDNA repeats (Dammann et al., 1993). The origins downstream of actively transcribed units are preferentially activated for replication (curved arrows; Pasero et al., 2000). Fob1 binds to the replication fork barrier (RFB) to prevent head-on collisions between the rightward moving replisome and the leftward moving RNA polymerases in the 35S transcription unit. C) Replication

652 of this section of chromosome is illustrated as a series of drawings at progressively later
653 times in S phase. The RFB/Fob1 complex enforces the mostly unidirectional replication
654 of this large region of Chr XII (Kobayashi and Horiuchi, 1996) with forks moving
655 leftward toward the centromere.

656 **Figure 2: Karyotyping the genome from aging chemostats using CHEF gel**
657 **electrophoresis**

658 A) Miniature aging chemostats allow us to isolate large populations of aging mother
659 cells. Magnetic beads are covalently bound to mother cells which are retained on the
660 chemostat wall by an external magnet while being continuously perfused with fresh
661 media to maintain a constant environment and to remove daughter cells. B) Viability of
662 mother cells was assessed with propidium iodide and flow cytometry (n > 10,000).
663 Dashed lines represent the second replicate population. C) Replicative age was
664 determined by manually counting bud scars of one mother population for each
665 genotype over time (n = 40 for each day). D and E) Ethidium bromide-stained CHEF
666 gels made from cells sampled across six days of growth from the two mother
667 populations of each of the three genotypes. Individual bands contain one or more
668 comigrating chromosomes. As cells age, additional DNA species become apparent.

669 **Figure 3: Characterizing individual chromosomes and rDNA structural forms in**
670 **aging *fob1Δ*, wild type and *sir2Δ* populations**

671 A and B) The autoradiograms of the CHEF gel shown in Fig 2D,E were produced by
672 Southern hybridization using fragments from *GAL3* and *CDC45* that identified the
673 positions in the gel of chromosomes IV and XII, respectively. Over the 6 days of
674 chemostat growth the intensity of the chr IV band diminishes while a smear of smaller

675 fragments increases. A similar disappearance of Chr XII occurs with appearance of the
676 same smear of smaller DNA fragments appearing near the end of each lifespan. C)
677 Hybridization using the rDNA specific probe reveals the age- and genotype-related
678 appearance of new bands migrating both slower and faster than Chr XII.
679 Simultaneously, there is a marked increase in rDNA signal in the well. D) Identification
680 of the new species of DNA bands that hybridize to the *NTS2* probe is revealed by
681 comparing their migration to known molecules in the gel: *H. wingei* and *S. cerevisiae*
682 chromosomes (not including *S. c.* Chr XII) from Fig 2D,E and the migration of
683 supercoiled (sc), nicked circular (nk) and linear (lin) forms of the 2 micron plasmid
684 (Supp Fig 6A). The labels of these rDNA specific bands in C were derived from this
685 log/linear plot. E) Tracings of *NTS2* hybridization on days 4 and 6 of the wild type
686 mothers reveals the relative amounts of the various forms of extrachromosomal rDNA.
687 Between days 4 and 6 the supercoils have been converted to nicked and linear species,
688 making their identification and quantification straightforward.

689 **Figure 4: Quantifying rDNA accumulation in aging populations**

690 A) For each day, the total signal intensity from *NTS2* (rDNA) and *CDC45* (Chr XII) was
691 divided by the total intensity from *GAL3*. This ratio was normalized to day 0 to
692 calculate fold change in probe intensity. B) Using the fold change of *NTS2* signal and
693 the days where replicative age increased from the previous day (WT: days 1 – 4, fob1:
694 days 1 – 6, sir2: days 1 – 3) we calculated the rate of rDNA copy number accumulation
695 using an exponential fit. C) The un-normalized intensity ratio of *NTS2*/*GAL3* is plotted
696 separately for DNA found in the well, full-length Chr XII, ERCs or fragments.

697 **Figure 5: Intrachromosomal recombination between two rDNA repeats that differ in**
698 **replication status**

699 A section of the rDNA locus with four repeats is shown with regions that have already
700 been replicated shaded in blue. A) The two rDNA repeats adjacent to RFBs 2
701 (replicated) and 4 (not yet replicated) undergo recombination. At the completion of
702 strand exchange one chromatid ends in a loop containing RFB3 with the replication fork
703 stalled at RFB2. The other chromatid has RFB1 adjacent to RFB4. B) After completion
704 of S phase, the top chromatid (B1) extends from the left telomere, through the
705 centromere ending in a stalled fork. The bottom chromatid (B2) has an unopposed
706 active fork that can continue replication toward the centromere through the previously
707 replicated region of the rDNA (runaway fork). C) The same two repeats engage in
708 recombination but in this case their replication status is reversed. D) After resolution of
709 the cross-over and completion of S phase, the top chromatid (D1) ends with an rDNA
710 loop containing RFBs 3 and 4; however, the fork that connects the loop to the right arm
711 of Chr XII is in the permissive orientation to replicate through RFBs that lie to its left
712 (rolling circle fork). The other chromatid (D2) remains branched with duplicated
713 centromeres and a fork blocked at RFB1.

714 **Figure 6: Mitotic consequences for mother cells with runaway or rolling circle forks**

715 If we assume that neither the runaway or rolling circle fork triggers a DNA damage or
716 mitotic checkpoint, the cell can continue into mitosis producing mother cells with
717 different fates. A) A mother cell that retains the truncated Chr XII will not survive due
718 to loss of essential genes. A mother cell that inherits the branched chromosome with
719 the runaway fork will survive but after replication in the next S phase the two cells will
720 each inherit a branched chromosome with a new runaway fork in the rDNA. B) The
721 branched chromosome contains sister chromatids that will create a bridge at mitosis
722 and be broken at or near the branch point in the rDNA. The chromatid with a rolling

723 circle fork lacks a centromere so it may segregate randomly. If the daughter inherits the
724 Chr XII fragment then the mother will either die from a loss of distal essential genes or
725 receive the complete copy of Chr XII that can be repaired by ligation across the single-
726 stranded interruption (Johansson and Diffley, 2021) and allow this mother cell to escape
727 a catastrophic outcome. If the mother inherits the Chr XII fragment then it can restore
728 the essential genes on Chr XII-right complementing the loss of those genes from the
729 centromere-proximal fragment. Subsequently a full-length chromosome could be
730 reconstructed from these two fragments but it will produce an rDNA-only rolling circle
731 lariat with a single-ended double stranded DNA break. The reciprocal product of this
732 division creates a mother cell with a full-length copy of Chr XII and the rolling circle
733 lariat containing second copies of all of the distal single copy genes. In the following S
734 phases, the rolling circle fork would continue synthesis and new runaway forks would
735 be produced. A multiply branched chromosome would be the result as the new forks
736 chase the preexisting forks along the lengthening lariat fragment.

737 **Figure 7: Extra copies of *MAS1* are found among Chr XII DNA fragments from dead**
738 **mother cells**

739 A) Quantification of the distribution of *CDC45* hybridization signal among different
740 forms of ChrXII in the CHEF gel blot from replicate 1 of the aging chemostat of *fob1Δ*,
741 wild type and *sir2Δ* strains. Most of the signals in days 1-4 remains in the well as a
742 consequence of branched chromosomal replication intermediates. In all three strains,
743 by day 6 more than half of the *CDC45* and *MAS1* signals are in fragments of 50-200 kb.
744 See Supp Fig 11A for data from replicate 2. B) The raw ratio of *MAS1* to *CDC45* among
745 DNA retained in the wells and the fragmented DNA was determined from the blots of
746 replicate 1 in Supp Fig 10A and Fig 3B. These un-normalized ratios are shown for the

747 days where more than 8.5% of the *CDC45* signal was found in fragmented DNA and
748 differed among the *fob1Δ*, wild type and *sir2Δ* strains. The data for replicate 2 are
749 shown in Supp Fig S11B. C) The raw ratio of *ARS1222* to *CDC45* on days 2 and 4 of four
750 wild type cultures is shown for DNA in the well and fragmented DNA. See Supp Fig 12
751 for images of the blot hybridized with *NTS2* (to detect ERCs as an indicator of relative
752 age of the population), *ARS1222* and *CDC45*.

753 **Figure 8**. **rDNA accumulation is heterogenous in aging populations**

754 A) Cell cycle distributions across the replicative lifespan of each population were
755 generated by staining fixed cells with Sytox green and measuring fluorescence intensity
756 with a flow cytometer (n > 10,000 cells). In addition to aging mother cells, we also
757 measured the cell cycle profiles of daughters of aging mothers (dashed distribution).
758 Day 0 cells were predominantly young mothers and had yet to produce daughters. The
759 x-axis was transformed from arbitrary fluorescence units to genomic content (N). The
760 1N and 2N peaks, corresponding to the genome before and after replication are present
761 in each plot. In mother cells, only a subset of cells appears to accumulate additional
762 DNA. Daughter cell cycle profiles do not show evidence of DNA accumulation. B) The
763 fraction of the population from the profiles shown in A (replicate 1) and in
764 Supplemental Figure 13 (replicate 2) with DNA content above 2.3N were quantified. C)
765 Mother cells from the *sir2Δ* population were collected on day 4 and sorted into live and
766 dead pools using fluorescence activated cell sorting (FACS) and the membrane
767 permeable stain, propidium iodide. A spot dilution assay was used to validate the
768 effectiveness of the sort. D) Cell cycle profiles from unsorted, live and dead cells
769 confirm that dead cells contain a higher fraction of the population with greater than
770 2.3N DNA content.

771 **SUPPLEMENTARY FIGURE LEGENDS:**

772 **Supplementary Figure 1:** Variation in rDNA copy number among clonal isolates

773 A) 28 colonies derived from isogenic stocks of *fob1Δ*, wild-type (WT) and *sir2Δ* cells
774 were grown from single cells and karyotyped by CHEF gel electrophoresis. Southern
775 blots of the CHEF gels were probed with *CDC45* to determine the size of Chr XII. B)
776 From the size of Chr XII we estimated the rDNA copy number of each of the 28 colonies
777 of each genotype shown in A. Dashed lines represent the starting rDNA copy number
778 for the aging time courses.

779 **Supplementary Figure 2: Pathways for the repair of single-ended, double-strand**
780 **breaks at the rDNA replication fork barrier**

781 A) Three complete repeats of the rDNA locus are shown after activation of the central
782 origin and migration of the bidirectional forks (green arrows) with the rightward fork
783 arrested at the replication fork barrier. Completion of replication of this region of the
784 rDNA locus depends upon a leftward moving fork from an origin located somewhere
785 to the right. A single stranded break on the leading strand template creates a single-
786 ended, double strand break that can engage three possible repair pathways: break
787 induced replication (BIR), replication fork restart (RFR), or homologous recombination
788 (HR). B) The most frequent pathway for repair of single ended DNA breaks is through
789 BIR (ref). The 3′ end (in this case the leading strand that was blocked at the RFB)
790 invades a homologous repeat and establishes a conservative form of replication,
791 characterized by the displacement bubble moving with the growing 3′ end of the
792 invading strand. However, in the rDNA this invading 3′ end immediately would be
793 blocked at the RFB. While this structure is unstable it could be resolved by the

794 incoming fork from an adjacent repeat. The number of rDNA repeats in this repaired
795 chromatid would depend on which repeat in the sister chromatid was used to initiate
796 BIR. C) Replication restart at a broken fork involves the formation of two separate
797 displacement loops initiated by each strand. This intermediate contains a Holliday
798 junction that is cleaved and repaired, resulting in reestablishment of semiconservative
799 replication at the new fork. That fork is again blocked but is stable and can be resolved
800 by an incoming fork from an adjacent repeat to the right. Depending on which repeat is
801 used for the initial invasion, the completed rDNA array may contain more or fewer
802 repeats. D) Homologous recombination, which involves breaking and rejoining of both
803 strands, does not repair a single ended break. E-G) The same three mechanisms of
804 repair can also occur intramolecularly with differing outcomes: BIR and RFR generate
805 fragments ending in lariat structures, resembling rolling circle replication intermediates,
806 while HR generates an ERC. E) The fork in the BIR lariat remains arrested at the RFB
807 and cannot extend into the adjacent sequence. The lariat is likely to be structurally
808 unstable resolving into the original linear fragment. F) The RFR lariat contains a
809 covalent circle, making it structurally more stable. The fork is again arrested at the RFB
810 and unable to use the circle as a replication template. As there is no incoming fork to
811 allow its resolution, it is likely to persist in this state. G) HR does not involve the
812 broken DNA end so the linear fragment remains unrepaired; however, it results in the
813 production of an ERC, with the number of repeats depending on which repeat was
814 chosen for the HR event. The major productive events and outcomes are highlighted in
815 green.

816 **Supplementary Figure 3: Southern blot analysis of replicate 2 aging populations**

817 The Southern blot of the second replicate CHEF gel was probed with *GAL3, CDC45* and
818 *NTS2* as in Figure 3A,B,C.

819 **Supplementary Figure 4**: **Southern blot analysis of Chr VIII and X in aging**
820 **populations**

821 The two CHEF gels shown in Figure 3D,E were sequentially probed with *CUP1* and
822 *ILM1*. (A and B are from replicate 1; C and D are from replicate 2.) While these probes
823 are present as a single chromosomal copy, both have also been seen to loop out and
824 form extrachromosomal circles (ECC). No evidence of ECC DNA was detected in aging
825 mothers.

826 **Supplementary Figure 5**: **Fragmented DNA fraction serves as a proxy for viability**

827 The fraction of signal in the range of fragmented DNA was quantified for *CDC45,*
828 *CUP1*, *GAL3,* and *ILM1*. The signal for fragmented DNA increases in a genotype
829 specific manner that mirrors changes in viability.

830 **Supplementary Figure 6**: **Quantification of the native 2-micron plasmid**

831 A) The CHEF gel for replicate 2 was probed with *FLP1* and used to confirm how
832 circular DNA migrates on CHEF gels and was used to identify forms of ERCs shown in
833 Fig 3D,E. B) We quantified the 2-micron signal by position in the gel—whether it was
834 retained in the well or whether it was able to migrate and normalized the signal relative
835 to *GAL3*. While there is a modest increase in total 2-micron over time, we do not see it
836 disproportionately accumulating in the well. We also note that the three genotypes
837 appear to maintain different copy numbers of 2-micron.

838 **Supplementary Figure 7**: **Quantification of signal in the well for *CUP1, ILM1, CDC45,***
839 **and *NTS2***

840 Chromosomes VIII and X were quantified using probes for *CUP1* and *ILM1*
841 respectively. Using either *CUP1* or *ILM1* to normalize rDNA amplification produced
842 similar results to those shown in Fig. 4A. While *GAL3* (Chr IV) was selected for the
843 chromosome to normalize against (Fig 4A), the analysis does not dramatically change if
844 we select either of these other single copy probes on other chromosomes.

845 **Supplementary Figure 8**: **Futcher model for 2-micron amplification**

846 The 6.3 kb 2-micron plasmid contains two 599 bp inverted repeats that partition the
847 plasmid into two unique loops—one that contains the origin of replication (ORI) and
848 the other that contains the *FLP1* gene. The plasmid exists in two isomeric forms (A and
849 B; form B is shown at the left) that differ in the orientation of one loop with respect to
850 the other. Their interconversion is catalyzed by the site-specific recombination activity
851 of Flp1 that recognizes the FRT site in each repeat. When recombination between
852 inverted repeats of differing replication status occurs, the two forks that would
853 normally meet at a site opposite the origin to terminate replication, are now moving in
854 the same direction around the 2-micron plasmid. As they chase each other around the
855 plasmid, they generate a loop of increasing length that is composed of multimers of the
856 2-micron plasmid. The Futcher model was the first example where recombination
857 between repeats of different replication status was proposed to lead to DNA
858 amplification. In the CICR model, we are proposing that recombination between *direct*
859 repeats in the rDNA also leads to the uncoupling of opposing replication forks. In this
860 case, the two forks are ultimately found on different DNA molecules without opposing
861 forks to complete replication. Redrawn from Futcher (1986).

862 **Supplementary Figure 9**: **Southern blot analysis of the region distal to the rDNA**
863 **using *MAS1* as the probe**

864 The CHEF gels shown in Figure 2D,E were probed with *MAS1*, a single copy sequence
865 located distal to the rDNA. (See Fig 1 for the positions of *MAS1* relative to the rDNA
866 and to *CDC45*.) Scans of the phosphor screens of the *MAS1* and *CDC45* blots were used
867 to quantify the hybridization signal in the well and chromosomal fragments. The
868 *MAS1*/*CD45* ratios are presented in Fig 7A.

869 **Supplementary Figure 10**: **Quantification of *CDC45* and *MAS1* hybridization of the**
870 **CHEF gel of replicate 2 of the aging chemostat**

871 See Figure 7A,B for a description of these data.

872 **Supplementary Figure 11**: **Southern blots of the CHEF gel with four replicates of**
873 **aging populations of wild type cells**

874 Four populations of wild type cells (S-1 through S-4) were aged for 4 days and the
875 samples analyzed by CHEF gel electrophoresis. The Southern blot was sequentially
876 hybridized with *NTS2* (A), *ARS1222* (B), and *CDC45* (C). The *ARS1222*/*CDC45* ratios
877 for days 2 and 4 are presented in Fig 7B.

878 **Supplementary Figure 12: Assessment of differences in copy number between the**
879 **rDNA-proximal and -distal regions of Chr XII**

880 A,B) Read-depth of Illumina sequence analysis across Chr XII from day 4 of aging
881 chemostat 1 compared to the day 0 sample. The sequences were aligned to version 3 of
882 the *S. cerevisiae* reference genome (Sac cer3) which has two copies of the rDNA
883 sequence. C,D) High resolution of read-depth across the single copy regions of Chr XII.

884 Note: the *CDC45* signal in the fragmented DNA for the wild type day 4 sample only
885 constitutes ~12 of the total signal (Fig 7A) and thus may not produce a significant copy
886 number change in the read-depth for the unfractionated sample that we sequenced.

887 **Supplementary Figure 13**: **rDNA accumulation in replicate 2 of the aging populations**

888 DNA content as a function of time and genotype was determined for replicate 2, as
889 described in Fig 8A. Mothers are indicated by filled histograms and daughters by open
890 histograms.

891 **Supplementary Figure 14**: **Live/dead FACS sort of replicate 2 mothers**

892 See Fig 8D for details.

893 **Supplementary Figure 15: Generation of unopposed replication forks by**
894 **intermolecular recombination between ERCs and the rDNA locus**

895 A) Chr XII is shown in mid-S phase with replication initiation having occurred within
896 the rDNA and in the flanking single copy sequences. The ERCs that is in the process of
897 replication is shown integrating into one of the replicated branches of the rDNA by
898 homologous recombination. Alternately, if the licensed ERC integrates, a subsequent
899 activation of its resident origin leads to the same intermediate that has bidirectional
900 forks with the leftward fork progressing toward the centromere and the rightward fork
901 being blocked at the RFB. Integration of either of these ERC forms into the unreplicated
902 portion of the rDNA locus only increases the length of the rDNA locus without creating
903 an imbalance of forks. B) By the end of S phase, no more licensed origins remain and
904 the single pair of bidirectional forks persist as there are no opposing forks to complete
905 replication termination. If these cells complete mitosis, neither cell would experience a
906 broken chromosome or an imbalance of proximal and distal single copy sequences. As

907 a result of its branched structure the top chromatid be retained in the well and
908 contribute an increase in rDNA signal in the well.

909 **Supplementary Figure 16: Overview of different modes of yeast aging**

910 Homologous recombination between rDNA repeats on the same chromatid can produce
911 either CICR events (left) or ERCs (right). The rates of these two forms of homologous
912 recombination may differ as CICR depends on the recombination occurring between
913 repeats of differing replication status and therefore can only occur during S phase.
914 ERCs could occur through the cell cycle. However, the time between the initial
915 recombination event and the time of death differ, as ERCs require many divisions to
916 accumulate to lethal levels while the consequences of CICR events are more proximal.
917 Loss of viability can also occur through mechanisms that do not involve the rDNA.

918 **REFERENCES:**

919 1. Amiama-Roig, A. *et al.* A Rfa1-MN–based system reveals new factors involved in the
920 rescue of broken replication forks. *PLOS Genetics* **21**, e1011405 (2025).

921 2. Aparicio, O. M., Billington, B. L. & Gottschling, D. E. Modifiers of position effect are
922 shared between telomeric and silent mating-type loci in *S. cerevisiae*. *Cell* **66**, 1279–1287
923 (1991).

924 3. Branzei, D. & Foiani, M. Regulation of DNA repair throughout the cell cycle. *Nat Rev*
925 *Mol Cell Biol* **9**, 297–308 (2008).

926 4. Brewer, B. J. & Fangman, W. L. A replication fork barrier at the 3′ end of yeast
927 ribosomal RNA genes. *Cell* **55**, 637–643 (1988).

928 5. Brewer, B. J. & Fangman, W. L. The localization of replication origins on ARS
929 plasmids in *S. cerevisiae*. *Cell* **51**, 463–471 (1987).

930 6. Choudhury, M., Zaman, S., Jiang, J. C., Jazwinski, S. M. & Bastia, D. Mechanism of
931 regulation of 'chromosome kissing' induced by Fob1 and its physiological significance.
932 *Genes Dev.* **29**, 1188–1201 (2015).

933 7. Defossez, P. A. *et al.* Elimination of replication block protein Fob1 extends the life
934 span of yeast mother cells. *Mol Cell* **3**, 447–455 (1999).

935 8. Futcher, A. B. Copy number amplification of the 2 μm circle plasmid of *Saccharomyces*
936 *cerevisiae*. *Journal of Theoretical Biology* **119**, 197–204 (1986).

937 9. Hattori, M., Horigome, C., Aspert, T., Charvin, G. & Kobayashi, T. Changed life
938 course upon defective replication of ribosomal RNA genes. *Genes Genet. Syst.* **97**, 285–
939 295 (2022).

940 10. Hendrickson, D. G. *et al.* A new experimental platform facilitates assessment of the
941 transcriptional and chromatin landscapes of aging yeast. *eLife* **7**, e39911 (2018).

942 11. Johansson, E.& Diffley, J. Unchecked nick ligation can promote localized genome re-
943 replication. *Current Biology*, 31, R710-R711

944 12. Kaeberlein, M., McVey, M. & Guarente, L. The Sir2/3/4 complex and Sir2 alone
945 promote longevity in *Saccharomyces cerevisiae* by two different mechanisms. *Genes Dev*
946 **13**, 2570–2580 (1999).

947 13. Kobayashi, T. & Horiuchi, T. A yeast gene product, Fob1 protein, required for both
948 replication fork blocking and recombinational hotspot activities. *Genes Cells* **1**, 465–474
949 (1996).

950 14. Kobayashi, T. A new role of the rDNA and nucleolus in the nucleus—rDNA
951 instability maintains genome integrity. *BioEssays* **30**, 267–272 (2008).

952 15. Kobayashi, T., Heck, D. J., Nomura, M. & Horiuchi, T. Expansion and contraction of
953 ribosomal DNA repeats in *Saccharomyces cerevisiae*: requirement of replication fork
954 blocking (Fob1) protein and the role of RNA polymerase I. *Genes Dev.* **12**, 3821–3830
955 (1998).

956 16. Kramara, J., Osia, B. & Malkova, A. Break-Induced Replication: The Where, The
957 Why, and The How. *Trends Genet* **34**, 518–531 (2018).

958 17. Li, S. *et al.* Microhomology-mediated end joining acts directly on replication forks to
959 repair single-ended double strand breaks. *Molecular Cell* **86**, 1230-1246 (2026)

960 18. Linskens, M. H. & Huberman, J. A. Organization of replication of ribosomal DNA in
961 *Saccharomyces cerevisiae*. *Mol Cell Biol* **8**, 4927–4935 (1988).

962 19. Liu, L. *et al.* Genome-wide screen reveals dependence of break induced replication
963 on several distinct checkpoints. *Nat Commun* **17**, 494 (2025).

964 20. Mortimer, R. K. & Johnston, J. R. Life Span of Individual Yeast Cells. *Nature* **183**,
965 1751–1752 (1959).

966 21. Morton, E. A. *et al.* Challenges and Approaches to Genotyping Repetitive DNA. *G3*
967 *(Bethesda)* **10**, 417–430 (2020).

968 22. Murray, J. A., Scarpa, M., Rossi, N. & Cesareni, G. Antagonistic controls regulate
969 copy number of the yeast 2 μm plasmid. *EMBO J* **6**, 4205–4212 (1987).

970 23. Rothstein, R. One-step gene disruption in yeast. in *Methods in Enzymology* vol. 101
971 202–211 (Academic Press, 1983).

972 24. Scherer, S. & Davis, R. W. Replacement of chromosome segments with altered DNA
973 sequences constructed in vitro. *Proceedings of the National Academy of Sciences* **76**, 4951–
974 4955 (1979).

975 25. Sinclair, D. A. & Guarente, L. Extrachromosomal rDNA Circles— A Cause of Aging
976 in Yeast. *Cell* **91**, 1033–1042 (1997).

977 26. Tsuchiyama, S., Kwan, E., Dang, W., Bedalov, A. & Kennedy, B. K. Sirtuins in Yeast:
978 Phenotypes and Tools. in *Sirtuins: Methods and Protocols* (ed. Hirschey, M. D.) 11–37
979 (Humana Press, Totowa, NJ, 2013).

980 27. van Brabant, A. J., Buchanan, C. D., Charboneau, E., Fangman, W. L. & Brewer, B. J.
981 An Origin-Deficient Yeast Artificial Chromosome Triggers a Cell Cycle Checkpoint.
982 *Molecular Cell* **7**, 705–713 (2001).

983 28. Ward, T. R. *et al.* Ribosomal DNA Replication Fork Barrier and HOT1
984 Recombination Hot Spot: Shared Sequences but Independent Activities. *Molecular and*
985 *Cellular Biology* **20**, 4948–4957 (2000).

986 29. Zakian, V. A., Brewer, B. J. & Fangman, W. L. Replication of each copy of the yeast 2
987 micron DNA plasmid occurs during the S phase. *Cell* **17**, 923–934 (1979).

988 30. Zylstra, A. *et al.* Senescence in yeast is associated with amplified linear fragments of
989 chromosome XII rather than ribosomal DNA circle accumulation. *PLOS Biology* **21**,
990 e3002250 (2023).

Figure 1

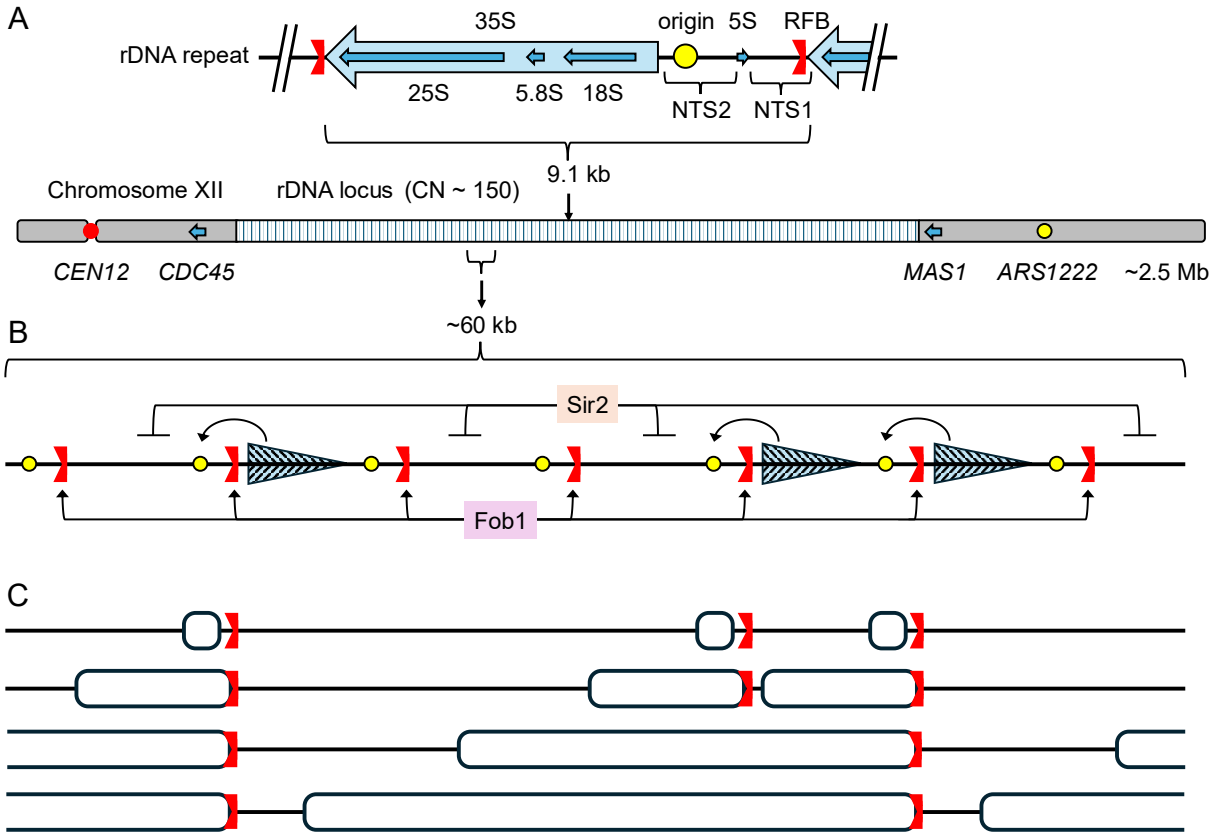
A
rDNA repeat
35S
origin
5S
RFB
25S
5.8S
18S
NTS2
NTS1
9.1 kb
Chromosome XII
rDNA locus (CN ~ 150)
CEN12
CDC45
MAS1
ARS1222
~2.5 Mb
~60 kb
B
Sir2
Fob1
C

Figure 2

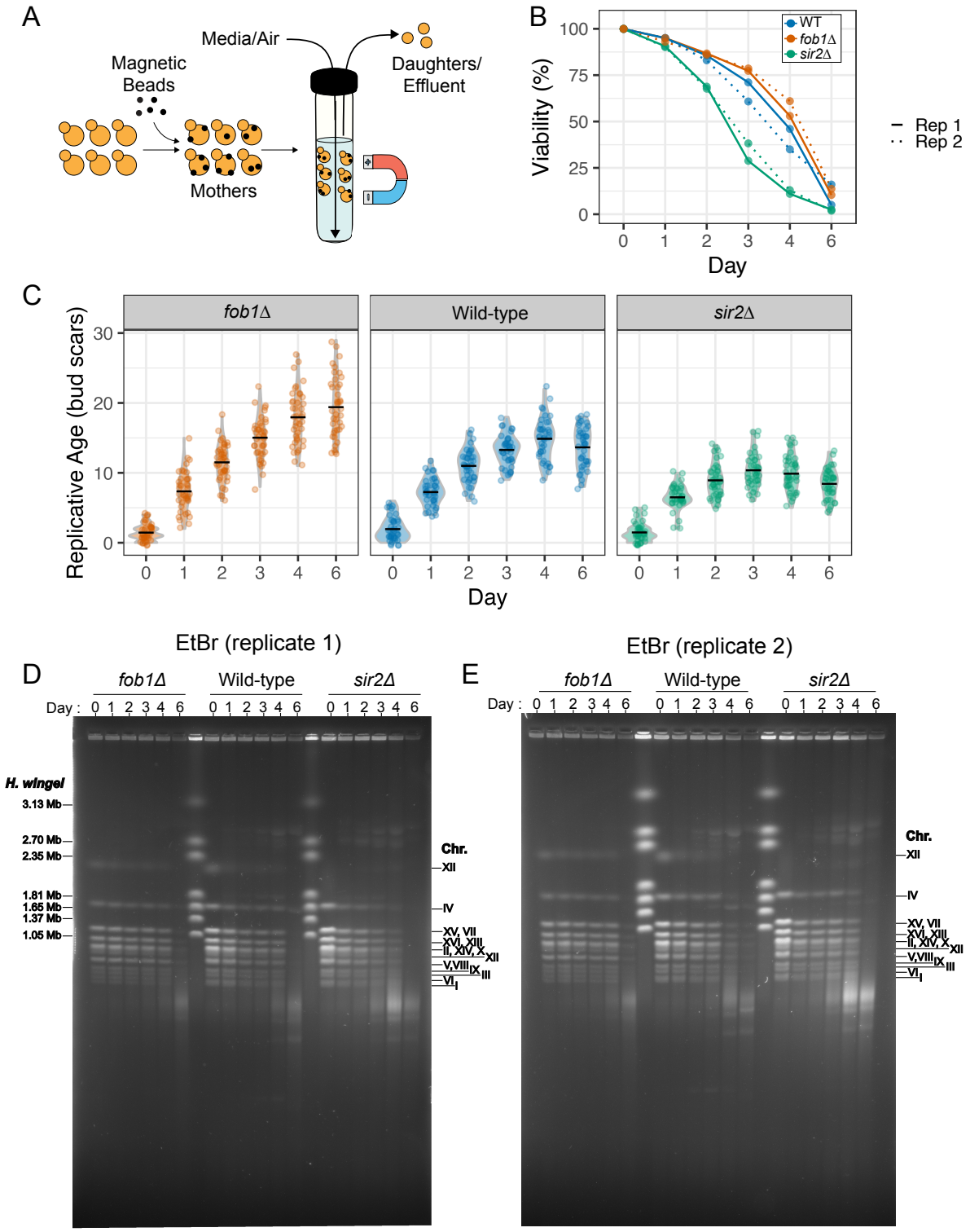
A
Media/Air
Magnetic Beads
Daughters/ Effluent
Mothers
B
Viability (%)
Day
WT
fob1Δ
sir2Δ
Rep 1
Rep 2
C
fob1Δ
Wild-type
sir2Δ
Replicative Age (bud scars)
Day
EtBr (replicate 1)
EtBr (replicate 2)
D
E
Day :
H. wingei
3.13 Mb
2.70 Mb
2.35 Mb
1.81 Mb
1.65 Mb
1.37 Mb
1.05 Mb
Chr.
XII
IV
XV, VII
XVI, XIII
II, XIV, X
V,VIII
IX
III
VI
I

Figure 3

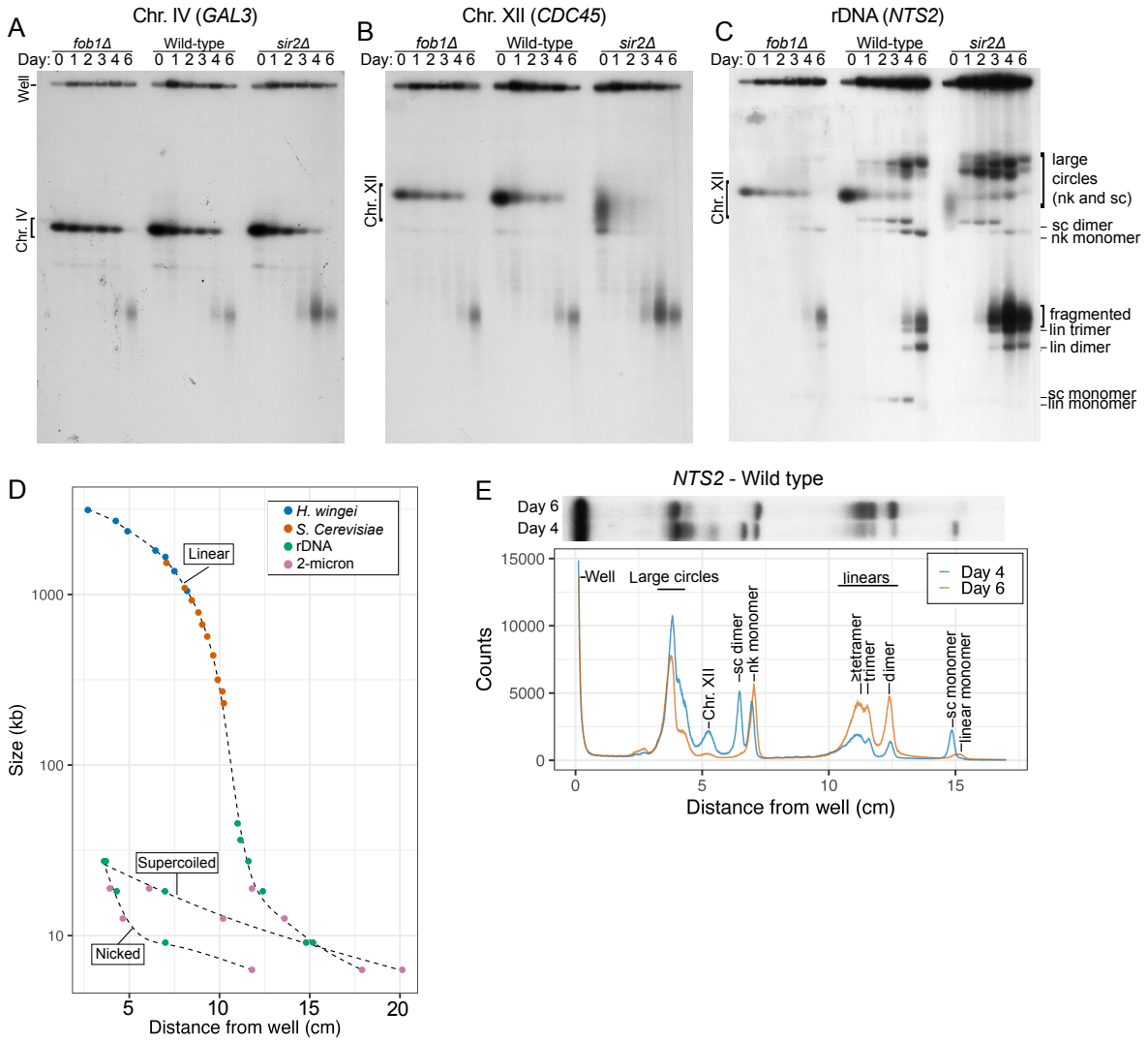
A
Chr. IV (GAL3)
fob1Δ
Wild-type
sir2Δ
Day: 0 1 2 3 4 6
Well
Chr. IV
B
Chr. XII (CDC45)
Chr. XII
C
rDNA (NTS2)
large circles (nk and sc)
sc dimer
nk monomer
fragmented
lin trimer
lin dimer
sc monomer
lin monomer
D
H. wingei
S. Cerevisiae
rDNA
2-micron
Linear
Supercoiled
Nicked
Size (kb)
Distance from well (cm)
E
NTS2 - Wild type
Day 6
Day 4
Counts
Well
Large circles
linears
Chr. XII
sc dimer
nk monomer
≥tetramer
trimer
dimer
sc monomer
linear monomer
Distance from well (cm)

Figure 4

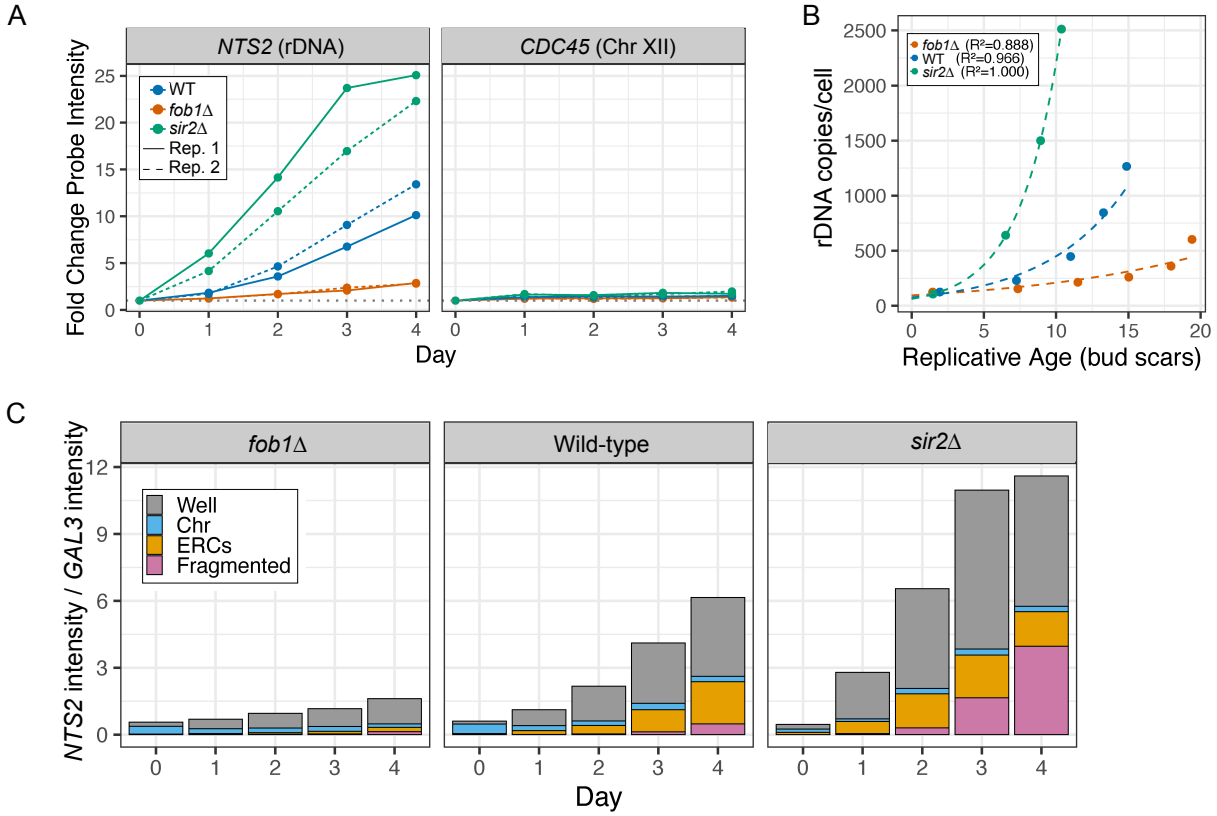
A
NTS2 (rDNA)
CDC45 (Chr XII)
Fold Change Probe Intensity
WT
fob1Δ
sir2Δ
Rep. 1
Rep. 2
Day
B
fob1Δ (R²=0.888)
WT (R²=0.966)
sir2Δ (R²=1.000)
rDNA copies/cell
Replicative Age (bud scars)
C
fob1Δ
Wild-type
sir2Δ
NTS2 intensity / GAL3 intensity
Well
Chr
ERCs
Fragmented
Day

Figure 5

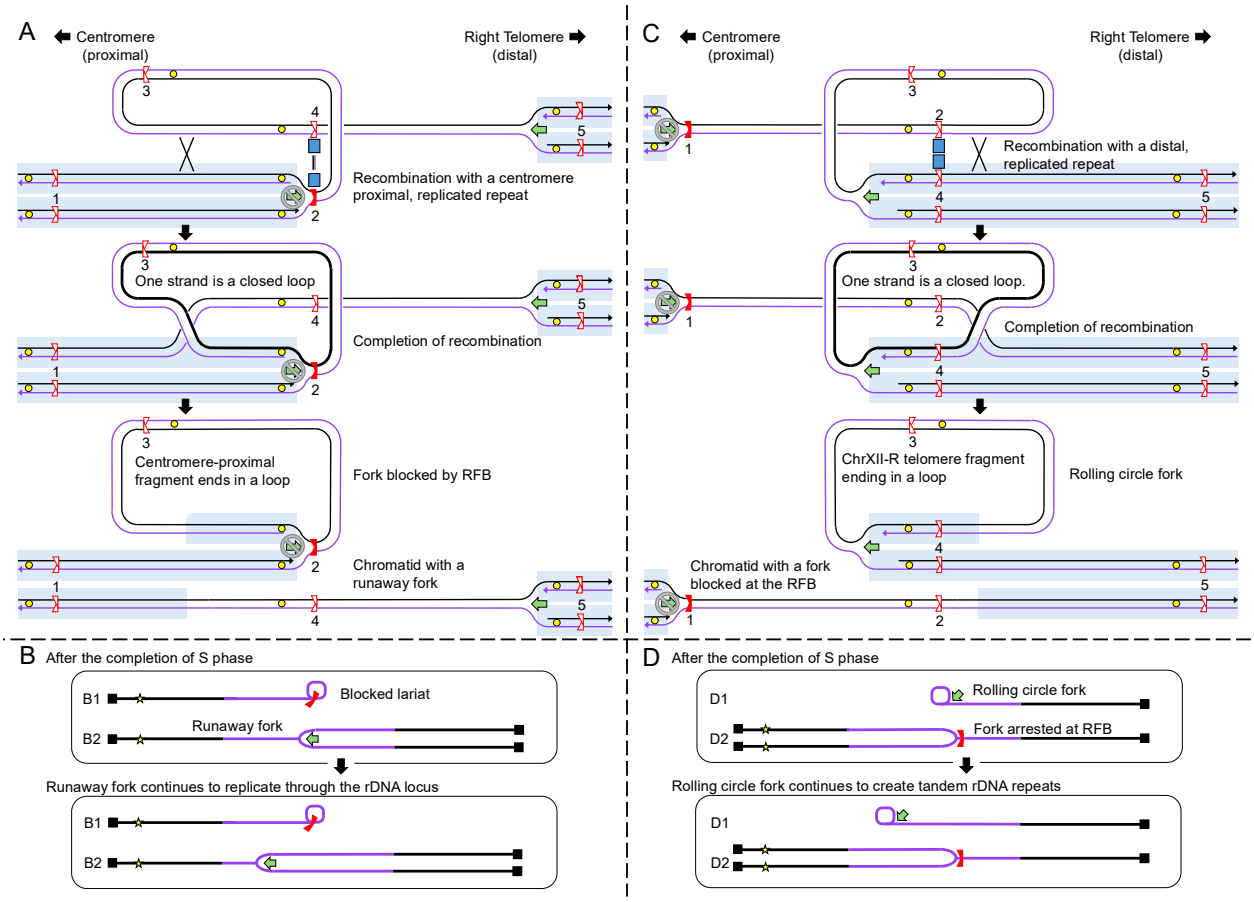
A
Centromere (proximal)
Right Telomere (distal)
Recombination with a centromere proximal, replicated repeat
One strand is a closed loop
Completion of recombination
Centromere-proximal fragment ends in a loop
Fork blocked by RFB
Chromatid with a runaway fork
C
Centromere (proximal)
Right Telomere (distal)
Recombination with a distal, replicated repeat
One strand is a closed loop.
Completion of recombination
ChrXII-R telomere fragment ending in a loop
Rolling circle fork
Chromatid with a fork blocked at the RFB
B After the completion of S phase
B1
B2
Blocked lariat
Runaway fork
Runaway fork continues to replicate through the rDNA locus
D After the completion of S phase
D1
D2
Rolling circle fork
Fork arrested at RFB
Rolling circle fork continues to create tandem rDNA repeats

Figure 6

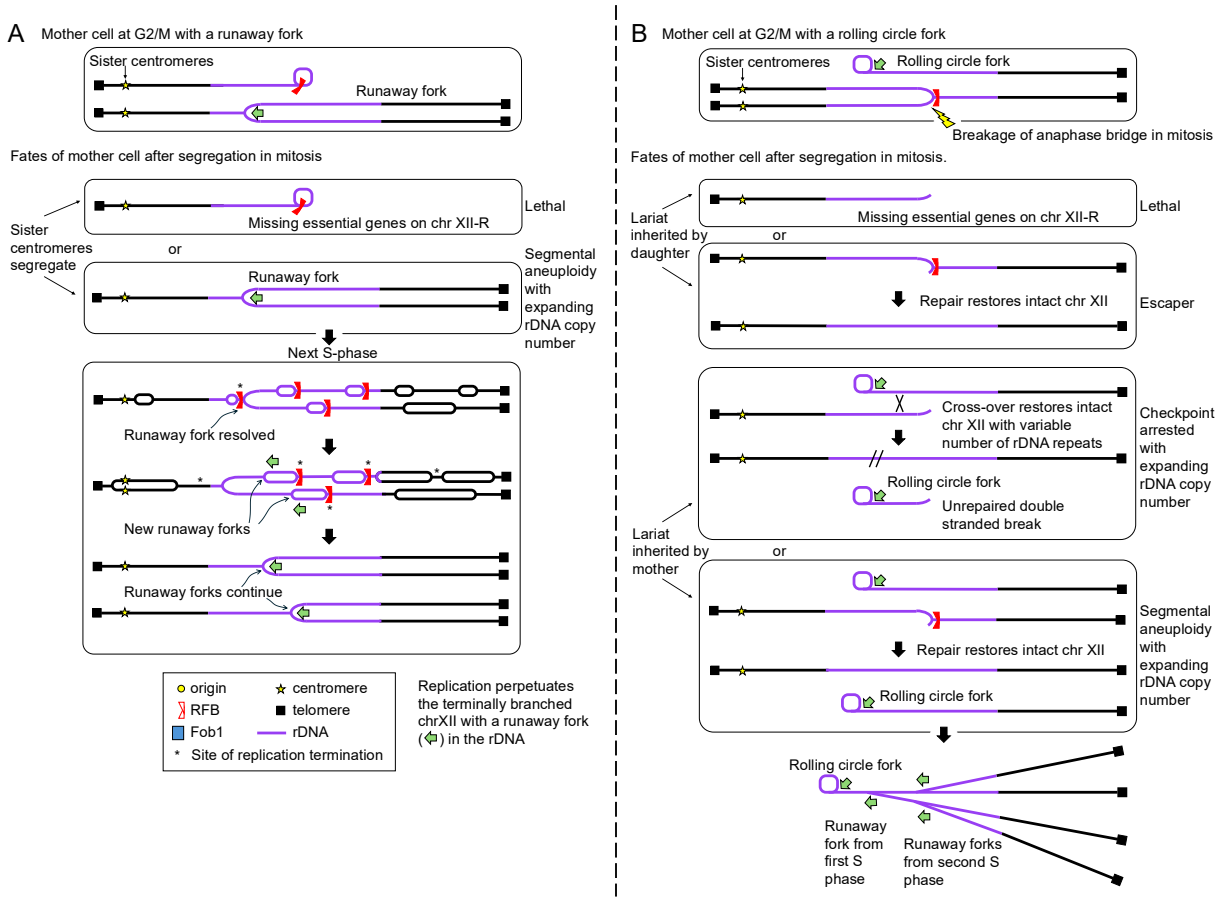
A
Mother cell at G2/M with a runaway fork
Sister centromeres
Runaway fork
Fates of mother cell after segregation in mitosis
Sister centromeres segregate
Missing essential genes on chr XII-R
Lethal
or
Runaway fork
Segmental aneuploidy with expanding rDNA copy number
Next S-phase
Runaway fork resolved
New runaway forks
Runaway forks continue
origin
centromere
RFB
telomere
Fob1
rDNA
Site of replication termination
Replication perpetuates the terminally branched chrXII with a runaway fork (⇦) in the rDNA
B
Mother cell at G2/M with a rolling circle fork
Sister centromeres
Rolling circle fork
Breakage of anaphase bridge in mitosis
Fates of mother cell after segregation in mitosis.
Lariat inherited by daughter
Missing essential genes on chr XII-R
Lethal
or
Repair restores intact chr XII
Escaper
Cross-over restores intact chr XII with variable number of rDNA repeats
Rolling circle fork
Unrepaired double stranded break
Checkpoint arrested with expanding rDNA copy number
Lariat inherited by mother
or
Repair restores intact chr XII
Rolling circle fork
Segmental aneuploidy with expanding rDNA copy number
Rolling circle fork
Runaway fork from first S phase
Runaway forks from second S phase

Figure 7

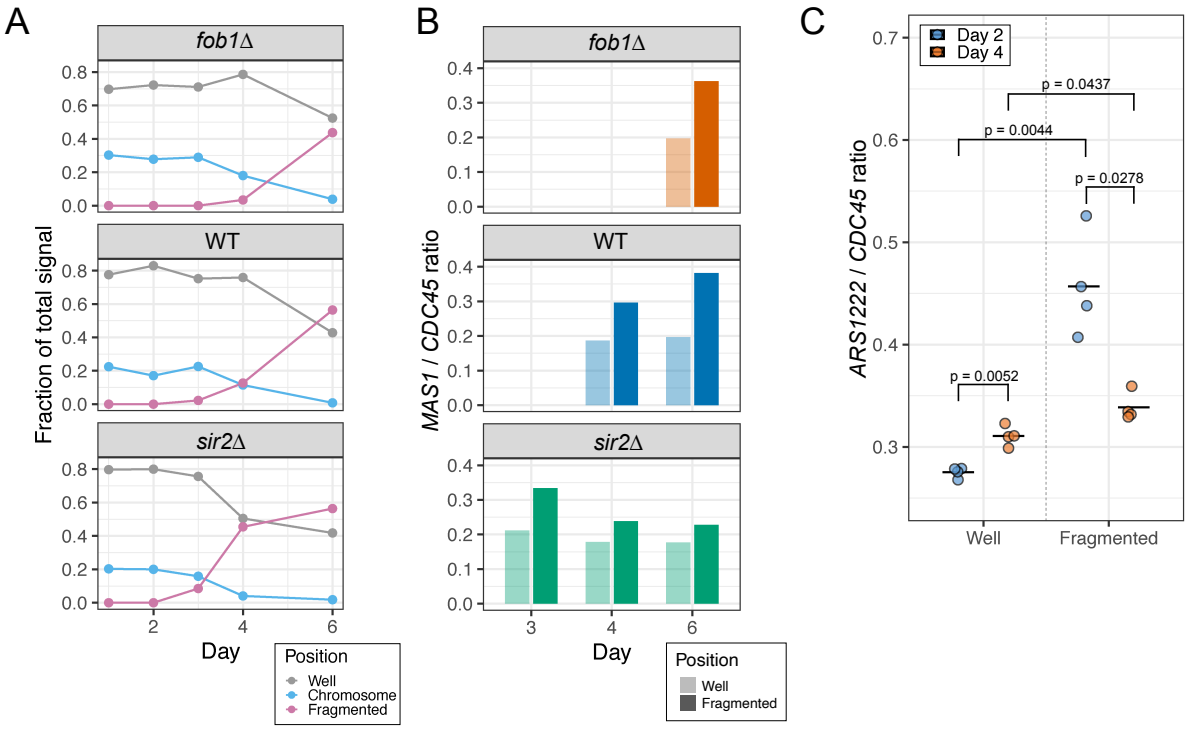
A
fob1Δ
WT
sir2Δ
Fraction of total signal
Day
Position
Well
Chromosome
Fragmented
B
fob1Δ
WT
sir2Δ
MAS1 / CDC45 ratio
Day
Position
Well
Fragmented
C
Day 2
Day 4
ARS1222 / CDC45 ratio
p = 0.0437
p = 0.0044
p = 0.0278
p = 0.0052
Well
Fragmented

Figure 8

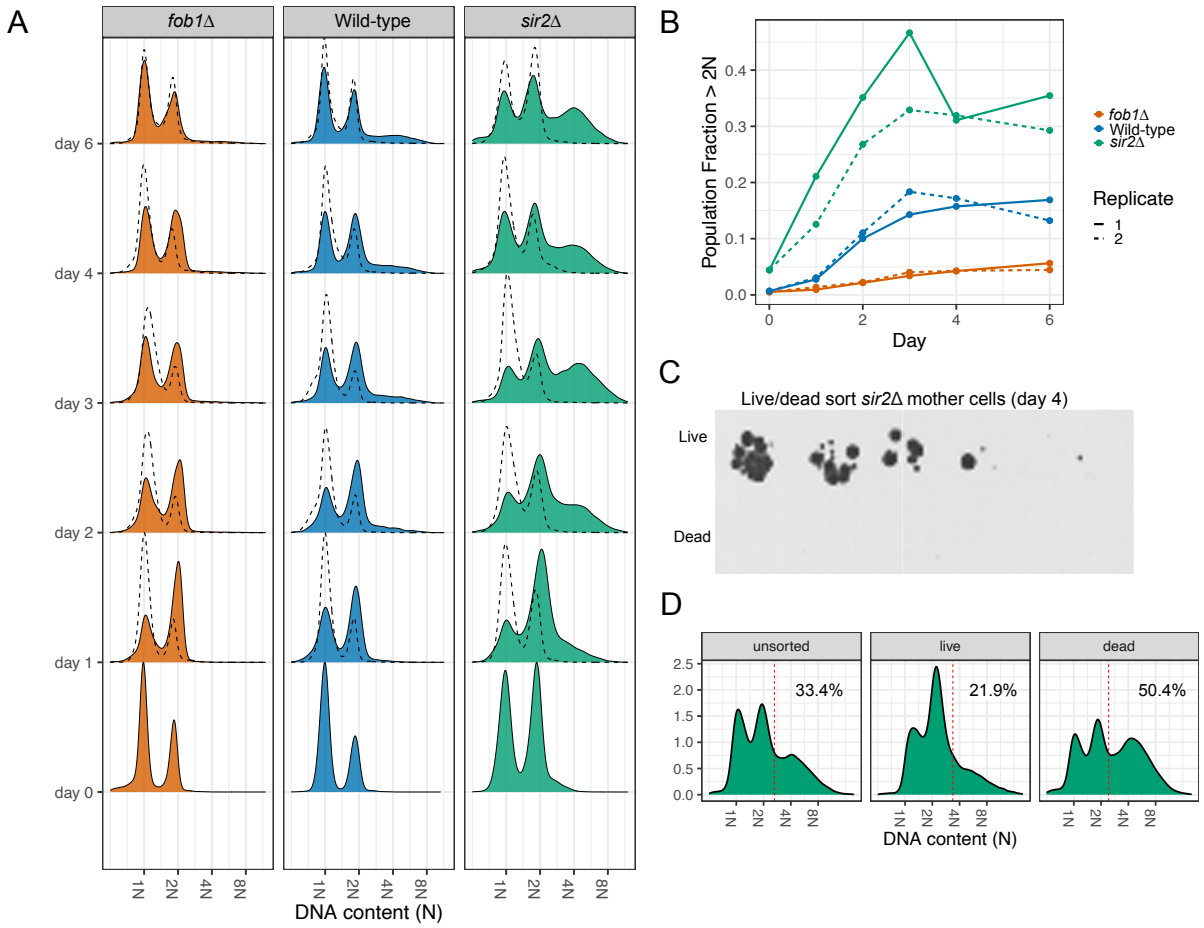
A
fob1Δ
Wild-type
sir2Δ
day 6
day 4
day 3
day 2
day 1
day 0
1N
2N
4N
8N
DNA content (N)
B
Population Fraction > 2N
0.0
0.1
0.2
0.3
0.4
0
2
4
6
Day
fob1Δ
Wild-type
sir2Δ
Replicate
1
2
C
Live/dead sort sir2Δ mother cells (day 4)
Live
Dead
D
unsorted
live
dead
33.4%
21.9%
50.4%
0.0
0.5
1.0
1.5
2.0
2.5
1N
2N
4N
8N
DNA content (N)